became comparable with that of human LF (Fig. 1). To exclude the possibility of cross-reactions between C-s3-33 and the anti-E2 antibody, we performed a Far-Western blot analysis in the absence of the E2 protein. No significant bands were obtained in this control experiment (Fig. 1). The Far-Western blot analysis using normal rat serum instead of anti-E2 antibody also detected no significant bands (data not shown). These results suggest that the specific E2 protein-binding activities of $(C\text{-}s3\text{-}33)_2$ and $(C\text{-}s3\text{-}33)_3$ increase with the degree of multiplication of C-s3-33.

$(C\text{-}s3\text{-}33)_2$ and $(C\text{-}s3\text{-}33)_3$ Efficiently Prevented HCV Infection in PH5CH8 Cells

Since we obtained the expected results that the E2-binding activities of $(C\text{-}s3\text{-}33)_2$ and $(C\text{-}s3\text{-}33)_3$ were stronger than that of C-s3-33, we next compared their anti-HCV activities in our HCV infection system using PH5CH8 cells (10, 25). The obtained result (Fig. 2) revealed that the anti-HCV activities of $(C\text{-}s3\text{-}33)_2$ and $(C\text{-}s3\text{-}33)_3$ (IC_{50} = 10 μM in both) became stronger than that of the C-s3-33 (IC_{50} = 23 μM), although their activities were somewhat weaker than that of human LF (IC_{50} = 5 μM). These results support the previous suggestion that the E2 protein-binding activity of C-s3-33 contributes to the inhibition of HCV infection (inoculum HCV-O) in human hepatocyte cells (25). However, in our HCV infection system, we failed to clearly show a difference in inhibiting activities between $(C\text{-}s3\text{-}33)_2$ and $(C\text{-}s3\text{-}33)_3$, because each standard deviation became somewhat large value due to the low level of cell culture-based HCV infection (20, 25, 31). In order to improve this point, we developed an infection system with VSVΔG*(HCV), a VSV pseudotype bearing the native E1 and E2 proteins derived from HCV-O (30), and this VSV pseudotype was used for further analysis as described below.

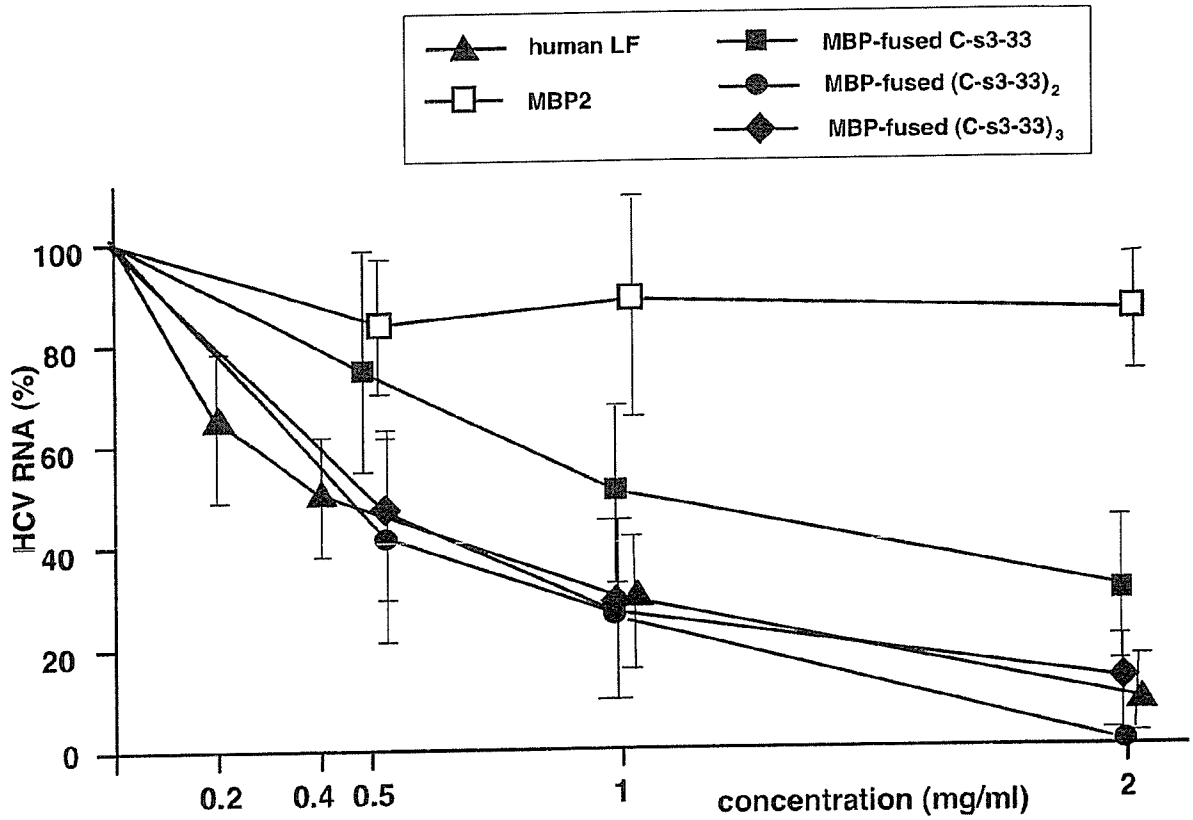

Fig. 2. Anti-HCV activities of MBP-fused C-s3-33, $(C\text{-}s3\text{-}33)_2$, and $(C\text{-}s3\text{-}33)_3$ in an HCV infection system using PH5CH8 cells. PH5CH8 cells and the inoculum HCV-O were used for the HCV-inhibiting assay, as described under "Materials and Methods." The number in the ordinate axis indicates the percent of HCV RNA determined by real-time LightCycler PCR (26). Approximately 2,000 copies of HCV RNA per μg of cellular RNA were reproducibly obtained using this HCV infection system (10, 26). In addition to the MBP-fused C-s3-33, $(C\text{-}s3\text{-}33)_2$, and $(C\text{-}s3\text{-}33)_3$, human LF and MBP2 were also used for the assay as control materials. The data are means ± SD of triplicates from three independent experiments.

Antiviral Effects of (C-s3-33)$_2$ and (C-s3-33)$_3$ against VSVΔG(HCV) Infection in PH5CH8 Cells*

Since PH5CH8 cells showed good susceptibility to our developed VSV pseudotype, VSVΔG*(HCV) (30), we examined the antiviral effects of (C-s3-33)$_2$ and (C-s3-33)$_3$ against VSVΔG*(HCV) infection in PH5CH8 cells, and compared them with those of the C-s3-33 and human LF. In this experiment, the antiviral effects of human TF and a C-s3-33-relevant fragment of human TF were also examined. The results (Fig. 3) clearly showed that human LF (IC_{50}=0.6 μM) strongly inhibited VSVΔG*(HCV) infection, but that human TF and the C-s3-33-relevant fragment of human TF did not, nor did MBP2, suggesting that inhibition against VSVΔG*(HCV) infection also occurred in an LF-specific manner as observed previously in the HCV infection system (25, 31). These results support previous findings (23, 30) using the VSV pseudotype infection system. Furthermore, we obtained clear results that C-s3-33 showed inhibiting activity against VSVΔG*(HCV) infection, and that its inhibiting activity was increased with multiplication of C-s3-33. The IC_{50} doses of C-s3-33, (C-s3-33)$_2$, and (C-s3-33)$_3$ were 17 μM, 5.0 μM, and 3.0 μM, respectively. This result indicates that antiviral activity of C-s3-33 is improved by the duplication and triplication of C-s3-33, although the antiviral activity of (C-s3-33)$_3$ is still weaker than that of human LF. We confirmed that these LF fragments did not inhibit VSVΔG*G (control virus without E1 and E2 proteins) infection in PH5CH8 cells (data not shown). In summary, our results suggest that direct interaction of the C-s3-33 fragment with the E2 protein in VSVΔG*(HCV) prevents the virus infection in PH5CH8 cells.

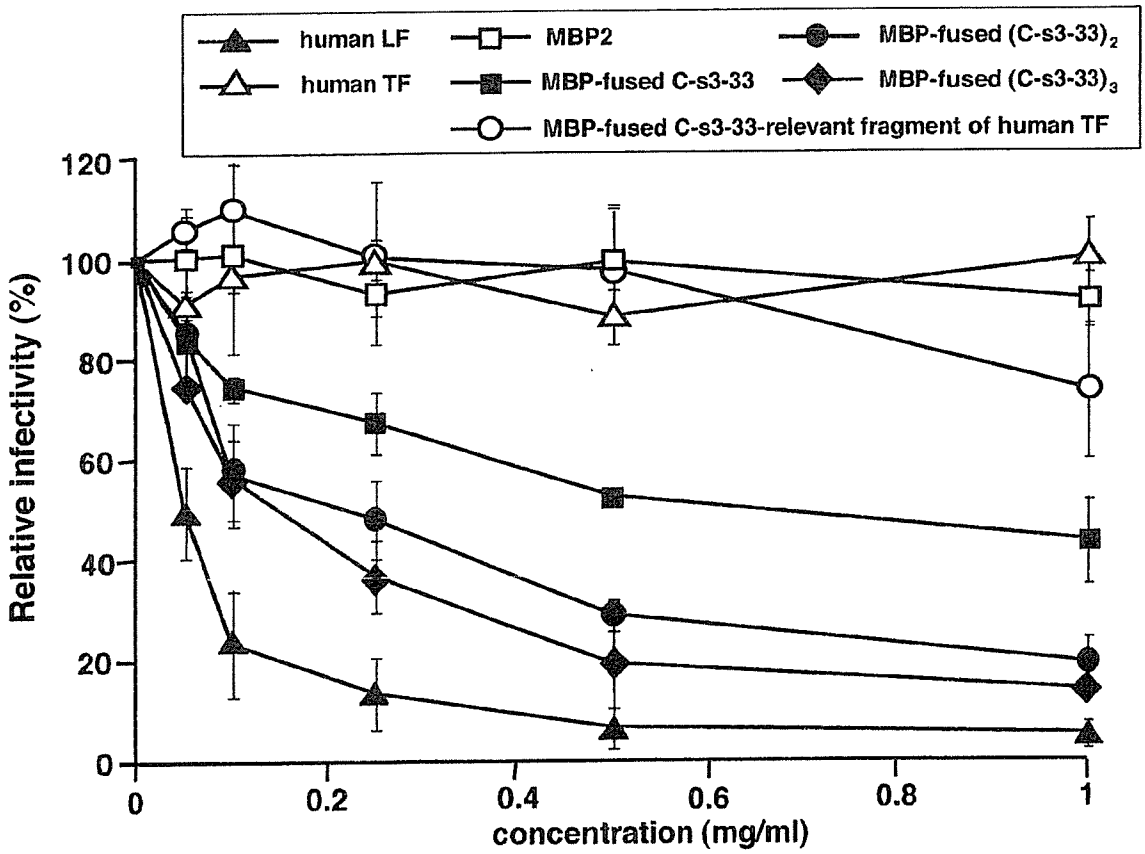

Fig. 3. Antiviral activity of the MBP-fused C-s3-33, (C-s3-33)$_2$, and (C-s3-33)$_3$ in the infection system of pseudotype virus using PH5CH8 cells. PH5CH8 cells and the VSV pseudotype, VSVΔG*(HCV), were used for the HCV-inhibiting assay, as described under "Materials and Methods." The number in the ordinate axis indicates the relative infectivity (%) calculated by counting GFP-positive cells. Approximately 100 GFP-positive cells per one assay were reproducibly obtained using this pseudotype infection system (30). In addition to the MBP-fused C-s3-33, (C-s3-33)$_2$, and (C-s3-33)$_3$, human LF, human TF, MBP2, and an MBP-fused C-s3-33-relevant fragment of human TF were also used for the assay as controls. The data are means ± SD of three independent experiments.

Antiviral Effects of $(C\text{-}s3\text{-}33)_2$ and $(C\text{-}s3\text{-}33)_3$ against VSVΔG(HCV) Infection in HepG2 Cells*

We have shown the inhibiting activities of LF fragments against HCV infection or VSV pseudotype infection in PH5CH8 cells; however, it is not clear whether or not the LF fragments used in this study show inhibiting activities against virus infection in cells other than PH5CH8 cells. To clarify this point, HepG2 cells were used for the analysis, because HepG2 cells showed the highest susceptibility to VSVΔG*(HCV) among 25 cell lines examined (30). As a consequence, we obtained similar results (Fig. 4) with those obtained in the infection system using PH5CH8 cells. The IC_{50} doses of C-s3-33, $(C\text{-}s3\text{-}33)_2$, and $(C\text{-}s3\text{-}33)_3$ were >12 μM, 7.6 μM, and 3.9 μM, respectively, indicating that, again, the inhibiting activity was increased with multiplication of C-s3-33, although antiviral activity of $(C\text{-}s3\text{-}33)_3$ was still weaker than that of human LF (IC_{50} = 1.2 μM). In conclusion, our results indicated that tandem repeats of C-s3-33 enhanced the inhibiting activity in cell culture-based HCV infection.

Discussion

In our previous (30) and present studies, we showed that pretreatment of VSV pseudotypes with bovine and human LFs reduced the infectivity of VSVΔG*(HCV) and VSVΔG*(E2) bearing only the E2 protein in a dose-dependent manner, whereas pretreatment with TF did not. In contrast, LFs partially inhibited the infectivity of VSVΔG*(E1) bearing only the E1 protein (30). These results suggested that the interaction of LF and the E2 protein is the main contributing factor to the prevention of HCV infection. This idea has been strongly supported by the results obtained in this study. We demonstrated that tandem repeats of C-s3-33, an anti-HCV peptide derived from human LF, enhanced the E2 protein-binding activity and the inhibiting activity

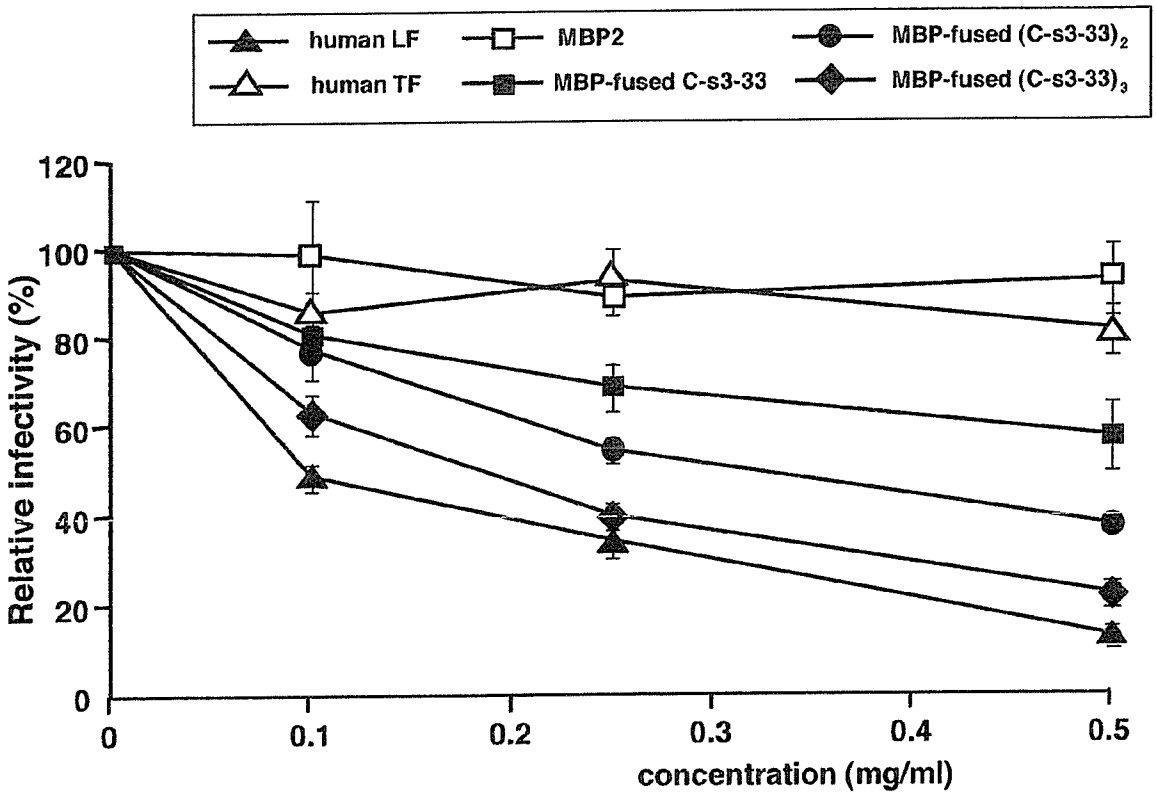

Fig. 4. Antiviral activity of the MBP-fused C-s3-33, $(C\text{-}s3\text{-}33)_2$, and $(C\text{-}s3\text{-}33)_3$ in the infection system of the pseudotype virus using HepG2 cells. HepG2 cells and the VSV pseudotype, VSVΔG*(HCV), were used for the HCV-inhibiting assay, as described in "Materials and Methods." The number in the ordinate axis indicates the relative infectivity (%) calculated by counting GFP-positive cells. Approximately 100 GFP-positive cells per one assay were reproducibly obtained using this pseudotype infection system (30). In addition to the MBP-fused C-s3-33, $(C\text{-}s3\text{-}33)_2$, and $(C\text{-}s3\text{-}33)_3$, human LF, human TF, and MBP2 were used for the assay as controls. The data are means ± SD of three independent experiments.

against infection by HCV or the VSV pseudotype, VSVΔG*(HCV), in human hepatic cell lines. These results strongly suggest that the direct interaction between C-s3-33 and the E2 protein plays a central role in the inhibition of HCV infection by LF.

Since C-s3-33 or repeated forms of C-s3-33 could prevent HCV and VSVΔG*(HCV) infection, C-s3-33 must bind to a region other than the region (aa 441–500 of E2 protein) required for heteromeric complex formation between E1 and E2 proteins. Our preliminary results suggested that the C-s3-33 bound to aa 411–500 and aa 600–661 of the E2 protein, indicating that the target sites of C-s3-33 may be plural. This result suggests a rather complex interaction between C-s3-33 and the E2 protein. To clarify this point, further comprehensive analysis will be needed.

Although tandem repeats of C-s3-33 enhanced the anti-HCV activity compared with that of the C-s3-33, the fact that their antiviral activities were still several-fold weaker than that of original human LF remains a subject to be resolved. As one approach to increase anti-HCV activity, tandem repeats of C-s3-33-relevant fragment of bovine LF may be useful, because we previously observed that the anti-HCV activity of bovine LF (IC_{50}=1.5 μM) was stronger than that of human LF (IC_{50}=5.0 μM) (26), and that the E2 protein-binding activity of the C-s3 (93 aa)-relevant fragment of bovine LF was stronger than that of C-s3 (25). Since 10 aa out of 33 aa differ between C-s3-33 and its relevant fragment of bovine LF, some aa substitutions between both fragments may help to further increase the anti-HCV activity of LF-derived peptides. Alternatively, some spacer between the C-s3-33 repeats may be needed. Therefore, further trials will be needed to achieve the maximum anti-HCV activity of C-s3-33.

In conclusion, the results of the present study demonstrated that tandem repeats of human LF-derived 33 aa prevented HCV infection more strongly than the 33 aa, and suggest that this repeated form will be useful as a novel anti-HCV reagent.

We thank T. Nakamura and A. Morishita for their technical assistance. This work was supported by a Grant-in-Aid for the Third-term Comprehensive 10-year Strategy for Cancer Control and by a Grant-in-Aid for research on hepatitis, both from the Ministry of Health, Labour, and Welfare, Japan; and by the Program for the Promotion of Fundamental Studies in Health Science of the Pharmaceutical and Medical Device Agency (PMAD), Japan. K.A. was supported by a Research Fellowship from the Japan Society for the Promotion of Science (JSPS) for Young Scientists.

References

1) Bartenschlager, R., and Lohmann, V. 2000. Replication of hepatitis C virus. J. Gen. Virol. **81**: 1631–1648.
2) Bartosch, B., Dubuisson, J., and Cosset, F.L. 2003. Infectious hepatitis C virus pseudo-particles containing functional E1-E2 envelope protein complexes. J. Exp. Med. **197**: 633–642.
3) Buonocore, L., Blight, K.J., Rice, C.M., and Rose, J.K. 2002. Characterization of vesicular stomatitis virus recombinants that express and incorporate high levels of hepatitis C virus glycoproteins. J. Virol. **76**: 6865–6872.
4) Cocquerel, L., Voisset, C., and Dubuisson, J. 2006. Hepatitis C virus entry: potential receptors and their biological functions. J. Gen. Virol. **87**: 1075–1084.
5) Farnaud, S., and Evans, R.W. 2003. Lactoferrin—a multifunctional protein with antimicrobial properties. Mol. Immunol. **40**: 395–405.
6) Feld, J.J., and Hoofnagle, J.H. 2005. Mechanism of action of interferon and ribavirin in treatment of hepatitis C. Nature **436**: 967–972.
7) Hijikata, M., Kato, N., Ootsuyama, Y., Nakagawa, M., and Shimotohno, K. 1991. Gene mapping of the putative structural region of the hepatitis C virus genome by *in vitro* processing analysis. Proc. Natl. Acad. Sci. U.S.A. **88**: 5547–5551.
8) Hijikata, M., Mizushima, H., Tanji, Y., Komoda, Y., Hirowatari, Y., Akagi, T., Kato, N., Kimura, K., and Shimotohno, K. 1993. Proteolytic processing and membrane association of putative nonstructural proteins of hepatitis C virus. Proc. Natl. Acad. Sci. U.S.A. **90**: 10773–10777.
9) Hsu, M., Zhang, J., Flint, M., Logvinoff, C., Cheng-Mayer, C., Rice, C.M., and McKeating, J.A. 2003. Hepatitis C virus glycoproteins mediate pH-dependent cell entry of pseudotyped retroviral particles. Proc. Natl. Acad. Sci. U.S.A. **100**: 7271–7276.
10) Ikeda, M., Nozaki, A., Sugiyama, K., Tanaka, T., Naganuma, A., Tanaka, K., Sekihara, H., Shimotohno, K., Saito, M., and Kato, N. 2000. Characterization of antiviral activity of lactoferrin against hepatitis C virus infection in human cultured cells. Virus Res. **66**: 51–63.
11) Ikeda, M., Sugiyama, K., Mizutani, T., Tanaka, T., Tanaka, K., Sekihara, H., Shimotohno, K., and Kato, N. 1998. Human hepatocyte clonal cell lines that support persistent replication of hepatitis C virus. Virus Res. **56**: 157–167.
12) Ikeda, M., Sugiyama, K., Tanaka, T., Tanaka, K., Sekihara, H., Shimotohno, K., and Kato, N. 1998. Lactoferrin markedly inhibits hepatitis C virus infection in cultured human hepatocytes. Biochem. Biophys. Res. Commun. **245**: 549–553.
13) Inudoh, M., Kato, N., and Tanaka, Y. 1998. New monoclonal antibodies against a recombinant second envelope protein of hepatitis C virus. Microbiol. Immunol. **42**: 875–877.
14) Inudoh, M., Nyunoya, H., Tanaka, T., Hijikata, M., Kato, N., and Shimotohno, K. 1996. Antigenicity of hepatitis C virus envelope proteins expressed in Chinese hamster ovary cells. Vaccine **14**: 1590–1596.
15) Ishii, K., Takamura, N., Shinohara, M., Wakui, N., Shin, H.,

Sumino, Y., Ohmoto, Y., Teraguchi, S., and Yamauchi, K. 2003. Long-term follow-up of chronic hepatitis C patients treated with oral lactoferrin for 12 months. Hepatol. Res. **25**: 226–233.

16) Iwasa, M., Kaito, M., Ikoma, J., Takeo, M., Imoto, I., Adachi, Y., Yamauchi, K., Koizumi, R., and Teraguchi, S. 2002. Lactoferrin inhibits hepatitis C virus viremia in chronic hepatitis C patients with high viral loads and HCV genotype 1b. Am. J. Gastroenterol. **97**: 766–767.
17) Kato, N. 2001. Molecular virology of hepatitis C virus. Acta Med. Okayama **55**: 133–159.
18) Kato, N., Hijikata, M., Ootsuyama, Y., Nakagawa, M., Ohkoshi, S., Sugimura, T., and Shimotohno, K. 1990. Molecular cloning of the human hepatitis C virus genome from Japanese patients with non-A, non-B hepatitis. Proc. Natl. Acad. Sci. U.S.A. **87**: 9524–9528.
19) Kato, N., Ikeda, M., Sugiyama, K., Mizutani, T., Tanaka, T., and Shimotohno, K. 1998. Hepatitis C virus population dynamics in human lymphocytes and hepatocytes infected *in vitro*. J. Gen. Virol. **79**: 1859–1869.
20) Kato, N., and Shimotohno, K. 2000. Systems to culture hepatitis C virus. Curr. Top. Microbiol. Immunol. **242**: 261–278.
21) Levay, P.F., and Viljoen, M. 1995. Lactoferrin: a general review. Haematologica **80**: 252–267.
22) Lonnerdal, B., and Iyer, S. 1995. Lactoferrin: molecular structure and biological function. Annu. Rev. Nutr. **15**: 93–110.
23) Matsuura, Y., Tani, H., Suzuki, K., Kimura-Someya, T., Suzuki, R., Aizaki, H., Ishii, K., Moriishi, K., Robison, C.S., Whitt, M.A., and Miyamura, T. 2001. Characterization of pseudotype VSV possessing HCV envelope proteins. Virology **286**: 263–275.
24) Noguchi, M., and Hirohashi, S. 1996. Cell lines from non-neoplastic liver and hepatocellular carcinoma tissue from a single patient. In Vitro Cell. Dev. Biol. Anim. **32**: 135–137.
25) Nozaki, A., Ikeda, M., Naganuma, A., Nakamura, T., Inudoh, M., Tanaka, K., and Kato, N. 2003. Identification of a lactoferrin-derived peptide possessing binding activity to hepatitis C virus E2 envelope protein. J. Biol. Chem. **278**: 10162–10173.
26) Nozaki, A., and Kato, N. 2002. Quantitative method of intracellular hepatitis C virus RNA using LightCycler PCR. Acta Med. Okayama **56**: 107–110.
27) Okada, S., Tanaka, K., Sato, T., Ueno, H., Saito, S., Okusaka, T., Sato, K., Yamamoto, S., and Kakizoe, T. 2002. Dose-response trial of lactoferrin in patients with chronic hepatitis C. Jpn. J. Cancer Res. **93**: 1063–1069.
28) Saito, I., Miyamura, T., Ohbayashi, A., Harada, H., Katayama, T., Kikuchi, S., Watanabe, Y., Koi, S., Onji, M., Ohta, Y., Choo, Q.L., Houghton, M., and Kuo, G. 1990. Hepatitis C virus infection is associated with the development of hepatocellular carcinoma. Proc. Natl. Acad. Sci. U.S.A. **87**: 6547–6549.
29) Tamura, T., Nozaki, A., Abe, K., Dansako, H., Naka, K., Ikeda, M., Tanaka, K., and Kato, N. 2005. cDNA microarray analysis of lactoferrin expression in non-neoplastic human hepatocyte PH5CH8 cells. Biochim. Biophys. Acta **1721**: 73–80.
30) Tamura, K., Oue, A., Tanaka, A., Shimizu, N., Takagi, H., Kato, N., Morikawa, A., and Hoshino, H. 2005. Efficient formation of vesicular stomatitis virus pseudotypes bearing the native forms of hepatitis C virus envelope proteins detected after sonication. Microbes Infect. **7**: 29–40.
31) Tanaka, K., Ikeda, M., Nozaki, A., Kato, N., Tsuda, H., Saito, S., and Sekihara, H. 1999. Lactoferrin inhibits hepatitis C virus viremia in patients with chronic hepatitis C: a pilot study. Jpn. J. Cancer Res. **90**: 367–371.
32) Thomas, D.L. 2000. Hepatitis C epidemiology. Curr. Top. Microbiol. Immunol. **242**: 25–41.
33) van der Strate, B.W., Beljaars, L., Molema, G., Harmsen, M.C., and Meijer, D.K. 2001. Antiviral activities of lactoferrin. Antiviral Res. **52**: 225–239.
34) Yi, M., Kaneko, S., Yu, D.Y., and Murakami, S. 1997. Hepatitis C virus envelope proteins bind lactoferrin. J. Virol. **71**: 5997–6002.

Journal of General Virology (2004), 85, 2397–2406 DOI 10.1099/vir.0.19578-0

Human T-cell leukaemia virus type I is highly sensitive to UV-C light

Akira Shimizu,[1,2] Nobuaki Shimizu,[1] Atsushi Tanaka,[1] Atsushi Jinno-Oue,[1] Bibhuti Bhusan Roy,[1] Masahiko Shinagawa,[1] Osamu Ishikawa[2] and Hiroo Hoshino[1]

Departments of Virology and Preventive Medicine[1] and Dermatology[2], Gunma University Graduate School of Medicine, 3-39-22 Showa-machi, Maebashi, Gunma 371-8511, Japan

Correspondence
Hiroo Hoshino
hoshino@med.gunma-u.ac.jp

Received 18 August 2003
Accepted 30 March 2004

The biological characteristics of human T-cell leukaemia virus type I (HTLV-I) are not yet well understood. UV light C (UV-C) sensitivity of HTLV-I was studied using a newly established infectivity assay: infection with cell-free HTLV-I dose-dependently induced syncytial plaques in cat cells transduced with the *tax1* gene of HTLV-I. HTLV-I was inactivated by a much lower UV dose than bovine leukaemia virus (BLV). The D_{10} (10% survival dose) of HTLV-I was about 20 J m^{-2}, while that of BLV was about 180 J m^{-2}, which was similar to the reported D_{10} of BLV. The UV sensitivity of HTLV-I and BLV was also examined by detecting viral DNA synthesis 24 h after infection. The D_{10} values determined by PCR using the *gag* primers for HTLV-I and BLV were close to those determined by the infectivity assays. Further PCR analyses were then performed to determine D_{10} values using several different primers located between the 5′-long terminal repeat (5′-LTR) and the *tax1* gene. The difference in UV sensitivity between HTLV-I and BLV was detected very early during replication, even during reverse transcription of the 5′-LTR of irradiated viruses, and became more prominent as reverse transcription proceeded towards the *tax1* gene. Chimeric mouse retroviruses that contain the LTR-*tax1* fragments of HTLV-I and BLV were made and hardly any difference in UV sensitivity was detected between them, suggesting that the difference was not determined by the linear RNA sequences of HTLV-I and BLV. HTLV-I was found to be much more sensitive than other retroviruses to UV.

INTRODUCTION

Human T-cell leukaemia virus type I (HTLV-I) was the first retrovirus discovered related to human diseases. It is the aetiological agent of adult T-cell leukaemia (Hinuma *et al.*, 1981; Poiesz *et al.*, 1980) and of HTLV-I-associated myelopathy or tropical spastic paraparesis (HAM/TSP) (Gessain *et al.*, 1985; Jacobson *et al.*, 1988; Osame *et al.*, 1986). The mechanism of entry of HTLV-I into cells or the reactivity of HTLV-I with human sera has frequently been investigated by using the vesicular stomatitis virus (VSV) pseudotype assay (Clapham *et al.*, 1984; Hoshino *et al.*, 1985), or by HTLV-I-specific PCR using concentrated HTLV-I (Fan *et al.*, 1992). As for the infectivity of HTLV-I, it has mainly been assessed by evaluating syncytium formation, in which HTLV-I-producing cells and non-infected cells are co-cultured (Hoshino *et al.*, 1983; Nagy *et al.*, 1983). However, virions of HTLV-I themselves, or cell-free HTLV-I, have rarely been used for examination of the infection mechanism. We have recently developed a new system by which we could detect syncytial plaque formation after infection of Tax1-expressing feline 8C cells with cell-free HTLV-I. In the present study, we examined the UV light C (UV-C) sensitivity of HTLV-I by this method. As we previously reported, the PCR system efficiently detects reverse-transcribed viral DNA in target cells after infection of cell-free HTLV-I (Haraguchi *et al.*, 1994). The UV sensitivity of HTLV-I was also investigated using this PCR system.

It has been known for a long time that retroviruses are, in general, more UV-resistant than other RNA viruses containing genomes of a similar length (Henderson *et al.*, 1992; Levinson & Rubin, 1966; Murphy & Gordon, 1981; Owada *et al.*, 1976). As for the dose required to reduce the infectivity to 10% (D_{10}), it has been reported that the D_{10} values of murine leukaemia virus (MuLV), bovine leukaemia virus (BLV) and human immunodeficiency virus type 1 (HIV-1) are 370, 220 and 280 J m^{-2}, respectively (Guillemain *et al.*, 1981; Yoshikura, 1989). Unexpectedly, we found that the D_{10} of HTLV-I was as low as about 20 J m^{-2} and that the reverse transcription of HTLV-I was a highly UV-sensitive stage. We investigated and discuss possible mechanisms that could explain the high UV sensitivity of HTLV-I.

METHODS

Cells. MT-2 (Miyoshi *et al.*, 1981), 8C/HTLV-I_{MEL5}, 8C/HTLV-I_{2M} and PG-4/HTLV-I_{MT-2} cells were used as HTLV-I-producing cells in

this study. The 8C/HTLV-I_{MEL5} and 8C/HTLV-I_{2M} cells are 8C cells (Fischinger *et al.*, 1973) derived from feline kidney cells persistently infected with HTLV-I_{MEL5} (Yanagihara *et al.*, 1991) and HTLV-I_{2M} derived from a Melanesian and a Japanese patient, respectively. PG-4/HTLV-I_{MT-2} cells were persistently infected with HTLV-I_{MT-2} derived from a Japanese patient and were newly established by co-culturing an HTLV-I_{MT-2}-producing rabbit T-cell line, Ra-1 (Miyoshi *et al.*, 1983), with a feline glial cell line, PG-4 (Haapala *et al.*, 1985). The 8C/HTLV-I_{2M} line c77 was a subclone of 8C cells that were co-cultivated with lethally irradiated ATL-2M cells producing HTLV-I_{2M} (Hoshino *et al.*, 1983). The BLV-producing cells were fetal lamb kidney (FLK) cells (van der Maaten & Miller, 1975). The indicator cells for infection with cell-free HTLV-I or BLV were 8C and 8C/Tax1. The 8C/Tax1 cells were derived from 8C cells transduced with the *tax1* gene of HTLV-I. When 8C cells had been transduced with a retroviral Tax-1-expression vector, DGL-Tax1 (Akagi *et al.*, 1991), they formed many syncytia after infection with HTLV-I produced by 8C/HTLV-I or PG-4/HTLV-I cells. Syncytium formation was inhibited by treatment with anti-HTLV-I seropositive human sera, a mouse mAb against HTLV-I gp46 or 3′-azido-3′-deoxythymidine (unpublished data). Details of this cell line will be described elsewhere. The indicator cells used for infection with chimeric Moloney murine leukaemia viruses (MoMuLVs) harbouring HTLV-I or BLV genome fragments were N4R (NP-2–CD4–ecoR). This is a cell line derived from NP-2 human glioma cells transduced with CD4 as well as an ecotropic MuLV receptor (Soda *et al.*, 1999). The packaging cells used for chimeric virus production were Phoenix-E cells (http://www.stanford.edu/group/nolan/). The 8C, 8C/Tax1, 8C/HTLV-I_{MEL5}, FLK and N4R cells were maintained in Eagle's minimum essential medium (E-MEM) containing 10% fetal calf serum (FCS). Phoenix-E cells were maintained in Dulbecco's modified MEM (D-MEM) containing 10% FCS. MT-2 cells were maintained in RPMI 1640 medium containing 10% FCS. The PG-4/HTLV-I_{MT-2} cells were maintained in McCOY'S 5A medium containing 15% FCS. All cells were maintained at 37 °C in a humidified, 5% CO_2 atmosphere.

Virus preparation. To prepare cell-free virus samples, 8C/HTLV-I_{MEL5}, 8C/HTLV-I_{2M}, PG-4/HTLV-I_{MT-2}, MT-2 and FLK cells were seeded at $6{\cdot}25 \times 10^5$ ml^{-1} and incubated for 2 days. Cells and debris were removed from the culture supernatants by low-speed centrifugation, and the supernatants were passed through 0·45 μm filters. The filtrates were dispensed into small aliquots and stored at −110 °C until use.

UV irradiation and dosimetry. Aliquots of 700 μl of supernatants that contained one of these virus samples was placed in the centre of a 35 mm plastic culture plate, kept on ice to eliminate thermal effects and gently agitated to ensure uniform irradiation. UV irradiation was carried out under a low-pressure mercury vapour lamp. The incident UV dose rate was determined using a spectroline DRC-100X dosimeter (Spectronics).

Determination of the UV sensitivities of HTLV-I and BLV. The 8C/Tax1 cells recently established by us were used for the infectivity assay. The 8C/Tax1 cells were seeded in 2 ml medium in flat-bottomed 6-well plates at $2{\cdot}5 \times 10^4$ cells ml^{-1}. The following day, after irradiation of the viruses with UV light, the cells were infected with 300 μl of HTLV-I or BLV preparations at 37 °C for 1 h in duplicate. The inocula were removed, the cells were washed once with culture medium and then fresh medium was added to the plates. The culture medium was changed at 3 and 6 days. The next day, the cells were fixed with methanol and stained with Giemsa solution and syncytial plaque were counted using an inverted microscope. Cells that contained more than four nuclei were considered to be syncytia and lesions that consisted of three or more syncytia were judged to be plaques. Syncytium numbers in control cultures were about 200 per well for each experiment. Variation of experimental data for each point was within 10% of corresponding mean value.

UV sensitivity of VSV. 8C cells were seeded into 35 mm plastic culture plates at $6{\cdot}0 \times 10^5$ cells ml^{-1}. The following day, VSV was inactivated with UV light and the cells were infected with 300 μl of VSV preparations at 37 °C for 1 h in duplicate. The cells were washed once with culture medium and medium containing agar was overlaid onto the plates. The next day, cells were stained with neutral red and numbers of plaques were counted using an inverted microscope.

UV sensitivity of cells. 8C, 8C/Tax1 or HeLa cells were seeded in 4 ml medium in 35 mm plastic culture plates at 500 cells ml^{-1}. The following day, after removal of the medium and irradiation of the cells with UV light at 0–12 J m^{-2}, fresh medium was added to the wells. After 7 days, cell colonies were counted.

UV sensitivities of HTLV-I and BLV determined by PCR. 8C cells were seeded in 1 ml medium in flat-bottomed 12-well plates at 2×10^4 cells ml^{-1}. Each virus was irradiated with UV. Target 8C cells were then infected with viruses at 37 °C for 1 h, washed with PBS once and incubated for 24 h as described previously (Haraguchi *et al.*, 1994; Yang *et al.*, 1994). The m.o.i. was about 1 for each virus. Cells were lysed with buffer that contained 10 mM Tris/HCl (pH 8·0), 1 mM EDTA, 0·45% NP-40 (Sigma), 0·45% Tween 20 (Sigma) and 20 mg protease K ml^{-1} (Sigma), incubated at 52 °C for 2 h and heated at 96 °C for 10 min to inactivate the protease K. To detect viral DNA by PCR, 15 μl reaction mixture that contained 10 mM Tris/HCl (pH 8·3), 50 mM KCl, 1·5 mM $MgCl_2$, each dNTP at 2 mM, 60 ng sense and antisense PCR primers and *Taq* DNA polymerase (Roche) was added to 5 μl cell lysate. PCR using the various primers shown in Figs 3(a) and 5(a) was performed in a thermal cycler (Perkin-Elmer Cetus). The PCR cycle was repeated 25–37 times under the following conditions: denaturation at 94 °C for 1 min, annealing at 55 °C for 45 s and extension at 72 °C for 1 min. Amplified products were then separated by electrophoresis in an agarose gel containing ethidium bromide as described elsewhere (Haraguchi *et al.*, 1994). We checked contamination of proviral DNA in virus inocula by PCR. No band was detected when PCR was done soon after inoculation of HTLV-I or BLV, indicating that neither proviral DNA in viral stocks nor strong stop DNA in virus stocks affected the results obtained. In addition to UV-irradiated viruses, cells were infected with serially diluted virus samples. We estimated the D_{10} by comparing the intensities of the PCR bands obtained with the UV-irradiated viruses with those bands obtained with diluted viruses, especially those obtained with the 1/10 dilution. That is, the intensity of each band was determined by densitometry and plotted on a semi-log graph and D_{10} values were determined using these graphs. D_{10} values determined using different PCR primers for a virus are expected to be dependent on the target size of UV irradiation. There should be an inverse proportional relationship between the D_{10} values and the target sizes of the virus genome examined, if the virus genome is homogeneously sensitive to UV. That is, the formula, $D_{10} \times$ target size (bp) = constant is expected to be pertinent to UV-inactivation of each virus. Expected data are shown using dotted lines in Figs 4 and 6.

PCR primers for HTLV-I and BLV. Oligonucleotide primers were synthesized (Hokkaido System Science) to detect reverse-transcribed DNA of HTLV-I and BLV. The names of the PCR primers, nucleotide sequences and orientation of the primers were as follows:

H-R-N, 5′-CGTCCGCCGTCTAGGTAAGTT-3′; H-U5-R, 5′-TGTGTTCTATGTTTCTCTCC-3′; H-gag-N, 5′-GGAGCCTTACCACACCTTCG-3′; H-gag-R, 5′-AGGCTGGACGACTAACACCTT-3′; H-pX1-N, 5′-CCACCCAGAGAACCTCTAAA-3′; H-pX2-N,

5′-TTGCATCTCCCCTTCGAAGA-3′; H-pX-R, 5′-GGGTGTACAGGTTTTGGGGC-3′; H-U3L-N, 5′-TGATACTGACTATGGGCC-3′; H-U3R-N, 5′-AGCGTGGAGACAGTTCAGGA-3′; B-R-N, 5′-CTTCTCCTGAGACCCTCGTG-3′; B-U5-R, 5′-TGTTTGCCGGTCTCTCCTGG-3′; B-gag-N, 5′-AACGGGTACCCTAACCCAACAA-3′; B-gag-R, 5′-GGGTTCCTTAGGACTCCGTC-3′; B-pX1-N, 5′-GGGATCCATTACCTGATAA-3′; B-pX2-N, 5′-TTCCCCGGGACTCCAATGAA-3′ and B-pX-R, 5′-TGGGTCTCGCAGGTGAGCGT-3′. The first H and B mean HTLV-I and BLV and the last N and R mean sense and antisense, respectively. The primer locations in the HTLV-I and BLV genomes are shown in Figs 3(a) and 5(a).

Construction of chimeric MoMuLVs. We constructed chimeric MoMuLVs that contain HTLV-I and BLV sequences as follows: fragments of HTLV-I or BLV were inserted into a MoMuLV genome vector containing the green fluorescent protein (GFP) gene after the *pol* region, pMX-GFP. When cells were infected with MoMuLVs containing the gene for GFP near the 3′ end of their genomes, GFP was expressed in the cells. That is, DNA fragments containing the pX(PPT)-U5 regions, i.e. from the polypurine tract (PPT) to U5 (823 bp) of HTLV-I and BLV, were obtained by PCR using the primer pairs H-pX2-N and H-U5-R, and B-pX2-N and B-U5-R, respectively. The fragments were cloned into the *Not*I site of the expression plasmid pMX-GFP to obtain the plasmids pMX-GFP-HTLV-I and pMX-GFP-BLV. They were transfected into Phoenix-E packaging cells for the production of recombinant ecotropic MoMuLVs and recombinant viruses were harvested. Recombinant viruses were irradiated with UV light as described above and N4R human cells expressing ecotropic MoMuLV receptors were infected with these viruses to detect GFP-expressing cells by flow cytometry (Cyto Ace-100).

UV sensitivities of chimeric pX(PPT)-U5 MoMuLVs. N4R cells were seeded at $2{\cdot}5 \times 10^4$ cells ml^{-1}. The next day, cells were infected with chimeric viruses in the presence of polybrene. Cells were incubated for 4 days and detached with trypsin and the infection level was determined by flow cytometry. About 30 % of cells were judged to be positive for GFP after infection of the non-irradiated chimeric viruses.

RESULTS

Infectivities of HTLV-I and BLV after UV irradiation

We determined the UV sensitivity of HTLV-I and compared it with that of BLV as a control. HTLV-I or BLV samples were placed in 35 mm plastic culture dishes, irradiated with UV and used to infect 8C/Tax1 cells. After 7 days, syncytial plaques were counted and the D_{10} values of these two viruses were determined (Fig. 1a).

For HTLV-I_{MEL5}, a Melanesian strain of HTLV-I, the number of syncytial plaques began to decrease at $1{\cdot}5$ J m^{-2} and was decreased to about half the number of plaques produced by the non-irradiated control at 5 J m^{-2}. This strain was almost completely inactivated at 27 J m^{-2}. For BLV, the number of syncytial plaques began to decrease at 45 J m^{-2} and was decreased to about half the number produced by the non-irradiated control at 70 J m^{-2}. BLV was almost completely inactivated at 270 J m^{-2}. The inactivation curve of HTLV-I decreased much more steeply with increasing UV dose than that of BLV (Fig. 1a). Thus,

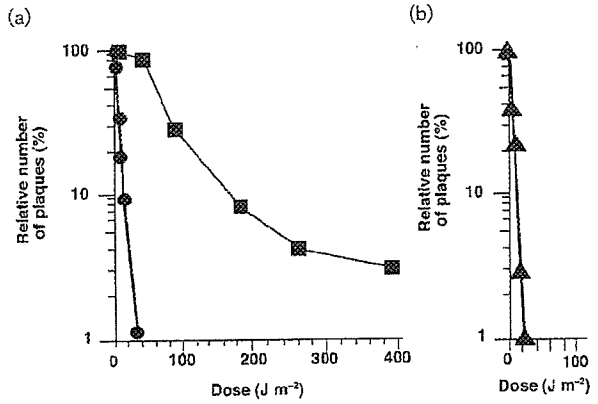

Fig. 1. UV sensitivities of HTLV-I and VSV. (a) UV sensitivity of HTLV-I. HTLV-I_{MEL5} and BLV were irradiated with UV and infected into 8C/Tax1 cells, and syncytial plaques were counted after 7 days. Syncytial plaque formation (number of plaques) by non-irradiated viruses is taken as 100 % and the relative numbers of syncytial plaques (%) formed by irradiated viruses are shown. In control culture dishes for HTLV-I and BLV, about 200 plaques were formed. Variation of experimental data for each point was within 10 % of corresponding mean value. The dose of UV irradiation is shown on the horizontal axis. Symbols: ●, HTLV-I; ■, BLV. (b) UV sensitivity of VSV. VSV is irradiated with UV and infected into 8C cells. Plaques were counted the following day. Plaque formation by non-irradiated viruses (about 200 plaques per well) is taken as 100 % and the relative numbers of plaques (%) formed by irradiated viruses are shown. The vertical axis shows the relative number of plaques.

HTLV-I was markedly more sensitive than BLV to UV and a large number of syncytia were observed even after irradiation of BLV at 45 J m^{-2} (Fig. 2). The D_{10} of HTLV-I was estimated to be about 17 J m^{-2}, while that of BLV was about 180 J m^{-2}. This value for BLV is similar to that reported previously, 220 J m^{-2} (Guillemain *et al.*, 1981), and those of other retroviruses (Guillemain *et al.*, 1981; Levinson & Rubin, 1966; Yoshikura, 1989). We also examined the UV sensitivities of two Japanese strains, HTLV-$I_{MT\text{-}2}$ and HTLV-I_{2M}, produced by PG-4/HTLV-$I_{MT\text{-}2}$ and 8C/HTLV-I_{2M} cells, respectively, as described above and found that their D_{10} values were also as low as about 20–30 J m^{-2} (data not shown).

UV sensitivity of VSV

We determined the UV sensitivity of VSV as a control. VSV samples were placed in 35 mm plastic culture dishes, irradiated with UV and infected into 8C cells. The next day, plaques were counted and the D_{10} of VSV was determined (Fig. 1b).

The number of plaques began to decrease at $2{\cdot}3$ J m^{-2} and almost completely inactivated at 14 J m^{-2}. The D_{10} of VSV was estimated to be about 6 J m^{-2} (Fig. 1b).

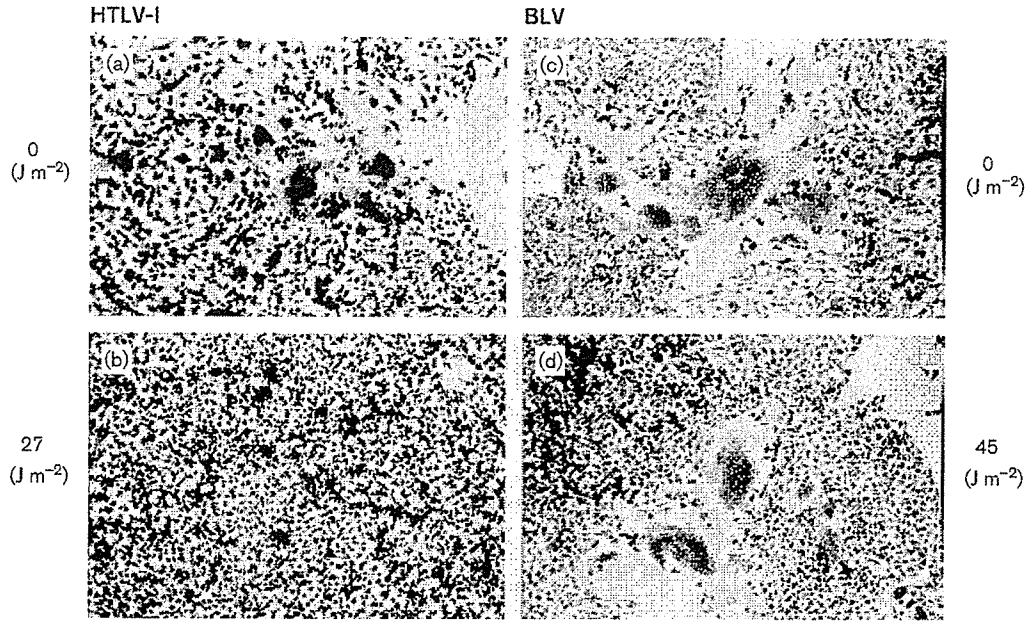

Fig. 2. Syncytial plaque formation by HTLV-I and BLV. HTLV-I_{MEL5} and BLV were irradiated at 0 and 27 J m^{-2}, and 0 and 45 J m^{-2}, respectively, and used to infect 8C/Tax1 cells. HTLV-I was almost completely inactivated by irradiation of 27 J m^{-2}, while BLV was not greatly inactivated even by 45 J m^{-2}. Syncytia formed by HTLV-I were smaller than those formed by BLV.

UV sensitivity of cells

HTLV-I and VSV were so UV-sensitive that we examined the UV sensitivity of the cells as a control. 8C cells were seeded and were irradiated the following day with UV light. After 7 days, we counted viable cell colonies and determined the D_{10} for colony formation of the cells. Colony formation of the 8C cells was completely inhibited at 6 J m^{-2} and the D_{10} of the 8C cells was about 3 J m^{-2} (data not shown). We also used 8C/Tax1 or HeLa cells for this assay and obtained similar results: their D_{10} values were about 3–5 J m^{-2}. Since these data were similar to those previously reported in normal lymphocytes and chronic lymphoid leukaemia lymphocytes (Bogdanov *et al.*, 1997), we considered our determination of UV dose to be accurate.

Viral DNA formation after infection of cells with UV-irradiated viruses

We examined whether the difference in UV sensitivity between HTLV-I and BLV could be detected shortly after infection, i.e. at the stage of reverse transcription. 8C cells were infected with HTLV-I_{MEL5} or BLV irradiated with UV and cell lysates were made 24 h later and examined for the formation of viral DNA by using PCR and *gag* primers (Fig. 3a, b) that were located in the region about 7·5 kb from the start of reverse transcription. In addition to UV-irradiated viruses, serially diluted virus samples were also used to infect the cells to determine quantitatively the D_{10} by PCR: representative results are shown in Fig. 3(c–f). Fig. 3(c–d) shows the effect of virus dilution on the PCR assay, and Fig. 3(e–f) shows the result of infection with irradiated viruses. The D_{10} values of the two viruses were estimated by comparing the intensities of the PCR bands obtained with the UV-irradiated viruses with those of the bands obtained with 1/10 diluted viruses (Fig. 3g, h). The D_{10} values of HTLV-I_{MEL5} and BLV were estimated to be 25 and 135 J m^{-2}, respectively. These data are similar to those determined with the infectivity assays (Fig. 1a). These findings revealed that the marked difference in UV sensitivity between HTLV-I and BLV was already detected at the reverse transcription step in which the negative strands of the virus genome are found.

We then used several PCR primer pairs located in different regions of the virus genome (Fig. 3a) and examined at which stage of reverse transcription a difference in D_{10} was initially detected. We plotted the D_{10} values determined by PCR using the *tax1* and *gag* regions of the PCR primers on a semi-log graph (Fig. 4). The difference in UV sensitivity between HTLV-I and BLV was even detected using PCR primers located in the *R-U5* region (Table 1). The curve for BLV declined gradually as reverse transcription proceeded, while that for HTLV-I declined steeply from the *tax1* gene to the *gag* gene and to the end of reverse transcription of the viral RNA (Fig. 4). As for HTLV-I, we noticed that there seemed to be an inverse relationship between D_{10} and the distance of the region examined from the start of reverse transcription, as shown by the dotted line in Fig. 4.

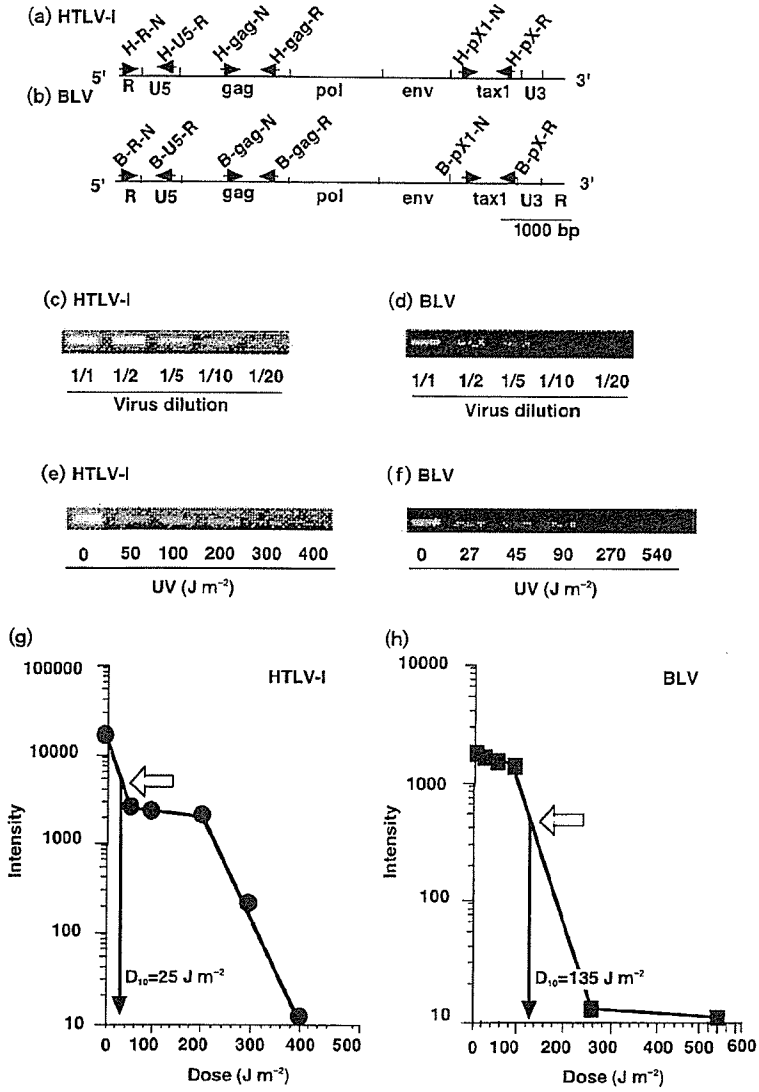

Fig. 3. Determination of D_{10} values using different PCR primers. (a)–(b) Locations of the PCR primers used in this experiment. (a) HTLV-I and (b) BLV sequence-specific primers. For the primers, H and B, and N and R mean HTLV-I and BLV and sense and antisense primer, respectively. A 1000 bp scale bar is shown. (c)–(f) Detection of viral DNA formation after infection of UV-irradiated viruses. 8C cells were infected with diluted (c–d) or UV-irradiated (e–f) HTLV-I_{MEL5} and BLV and cultured for 24 h. Viral DNA was detected by PCR (30 cycles) using the *gag* primers in Fig. 3(a). The five lanes of (c)–(d) were obtained using virus dilutions from 1/1 to 1/20. The six lanes of (e)–(f) were obtained using virus irradiated at dose from 0 to 400 J m^{-2} for HTLV-I_{MEL5} and from 0 to 540 J m^{-2} for BLV. (g)–(h) Densitometry of PCR bands. PCR bands were subjected to densitometry and their intensities are shown using arbitrary units. Open arrows show the intensities that the 1/10 diluted viruses gave upon PCR and closed arrows show D_{10} values. D_{10} values for HTLV-I_{MEL5} and BLV were estimated to be 25 and 135 J m^{-2}, respectively.

UV sensitivity of viral DNA formation in the early stages of reverse transcription

We further investigated the early stages of reverse transcription of the HTLV-I RNA genome more precisely, as there was a marked difference in UV sensitivity between HTLV-I and BLV even when *R-U5* or *tax1* primers were used (Fig. 4; Table 1). We used an antisense primer, H-U5-R, and four sense primers, H-R-N, H-U3R- N, H-U3L-N and H-pX2-N, corresponding to different positions to change the length of the amplified DNA (Fig. 5a, b): thus the expected PCR fragments were calculated to be 300, 423, 754 and 823 bp, respectively. Cells were infected with serially diluted virus samples in addition to UV-irradiated viruses to determine quantitatively the D_{10} by PCR (Fig. 5c, d) as described above. Irradiation at 150 J m^{-2} was estimated to be necessary to reduce the intensity of the PCR band for HTLV-I to 1/10 (D_{10}) of the control level (Fig. 5c), while 360 J m^{-2} was necessary for BLV (Fig. 5d). An apparent difference in D_{10} values between HTLV-I and BLV was detected at the stage of reverse transcription of the *U5-R* region. After that, the D_{10} of HTLV-I was markedly decreased, while the D_{10} of BLV did not considerably change (Fig. 6). As for the D_{10} values of HTLV-I, determined by using the four different PCR primers, that is 365, 220, 200 and 150 J m^{-2}, there again seemed to be an inverse relationship between these values and the target sizes of viral RNA detected by PCR. The D_{10} of BLV determined by the use of the B-pX2-N primer, shown by the solid line, was much higher than the predicted value, shown by the dotted line (Fig. 6), suggesting that the D_{10} for BLV was not proportional to the target size of viral RNA irradiated or that the UV-irradiated genome of BLV would be repaired during reverse transcription.

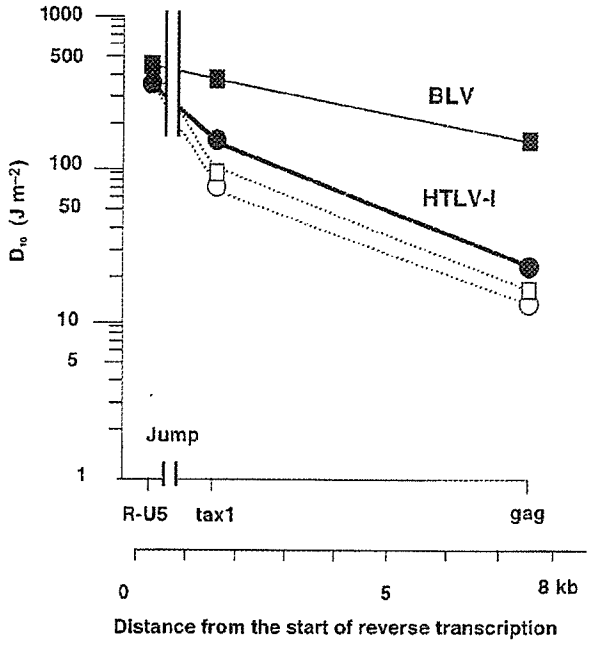

Fig. 4. D_{10} values determined by using various PCR primer pairs. The horizontal axis shows the distance from the beginning of reverse transcription (target size of UV irradiation) and the locations of the primers used. Experiments were repeated at least twice. Mean D_{10} values were plotted using closed symbols. The first-strand transfer (jump) occurs in the *R* region (between *U5* and *tax1*). An apparent difference in the D_{10} values between HTLV-I and BLV was even detected at an early stage of reverse transcription. The D_{10} values for the *tax1* and *gag* regions were calculated, shown by open symbols, on the assumption that there is an inverse relationship between the distance of PCR primer locations in the virus genomes from the start of reverse transcription and the D_{10} values determined by using the corresponding PCR primers. These calculated values were plotted using open symbols with dotted lines. Symbols: ● and ○, HTLV-I; ■ and □, BLV.

Table 1. Summary of the UV sensitivity of HTLV-I and BLV

HTLV-I_{MEL5} and BLV were irradiated with UV and their D_{10} values were determined by infectivity (syncytial plaque formation in 8C/Tax1 cells) and PCR assays (8C cells) as described in Methods. The D_{10} values of DNA formation determined using the *gag* PCR primers were similar to those determined by the infectivity assay. The target sizes of UV irradiation and their D_{10} values determined using HTLV-I but not BLV seemed to be in inverse proportion. The D_{10} values of BLV determined by PCR for *R-U5* or *tax1* were much smaller than expected from the results of the infectivity assay.

Parameter	Target size (kb)	HTLV-I	BLV
Infectivity	8·5	17±6*	180±1
PCR			
R-U5	0·3	370±90	480±170
tax1	1·5	150±40	400±57
gag	7·5	28±4	195±85

*D_{10}, Mean±SD (J m^{-2}).

UV sensitivity of the pX(PPT)-U5 region of HTLV-I and BLV

Since a marked difference in the UV sensitivity of HTLV-I and BLV was apparent during reverse transcription of the *U5-tax1* region (Figs 4 and 6), we investigated whether the difference in UV sensitivity between the HTLV-I and BLV genomes was due to differences in their RNA sequences in this region. Therefore, we constructed chimeric MoMuLVs (MoMuLV GFP-HTLV-I and MoMuLV GFP-BLV) by inserting an 823 bp sequence of HTLV-I or BLV, pX(PPT)-U5, into pMX-GFP to produce MoMuLV GFP chimeric viruses. In these viruses, most of the MoMuLV genome RNA would be reverse transcribed after HTLV-I and BLV pX(PPT)-U5 RNA.

Recombinant viruses were irradiated with UV and inoculated into N4R cells. Fluorescent cells were detected by flow cytometry 4 days after infection. The proportions of GFP-positive N4R cells infected with non-irradiated MoMuLV GFP, MoMuLV GFP-HTLV-I and MoMuLV GFP-BLV were 35, 23 and 20 %, respectively. Next, each virus was irradiated at 20, 100 and 500 J m^{-2} and used to infect N4R cells. The proportions of GFP-positive N4R cells were, 26, 17 and 0·9 % for MoMuLV GFP, 19, 13 and 1·0 % for MoMuLV GFP-HTLV-I and 16, 9 and 0·6 % for MoMuLV GFP-BLV, respectively, indicating that the three viruses were similarly inactivated in proportion to the irradiation dose. The D_{10} values of these three viruses were calculated to be about 420 J m^{-2} and were similar to the reported D_{10} of MoMuLV, 370 J m^{-2}, determined by an infectivity assay (Guillemain *et al.*, 1981). We concluded that no special UV-sensitive sequence was present in the 823 bp of the pX (PPT)-U5 regions of HTLV-I and BLV.

DISCUSSION

The UV sensitivity of RNA viruses has long been studied (Murphy & Gordon, 1981), but the mechanism of UV inactivation is still not clear. There have been several reports on the mechanisms of UV inactivation in retroviruses: retroviruses are much more resistant than other RNA viruses to UV, if the size of their RNA genomes is considered (Henderson *et al.*, 1992; Levinson & Rubin 1966; Owada *et al.*, 1976; Yoshikura, 1989). In our experiments, the D_{10} values for VSV and BLV determined by infectivity assays were found to be about 6 and 180 J m^{-2}, in agreement with reported values, although their genomic RNAs are of a similar size. It is not yet known why retroviruses are so UV resistant. It has also not yet been determined which part of retrovirus virions or which step of the virus replication cycle is most sensitive to UV irradiation. HTLV-I and BLV each contain two pairs of

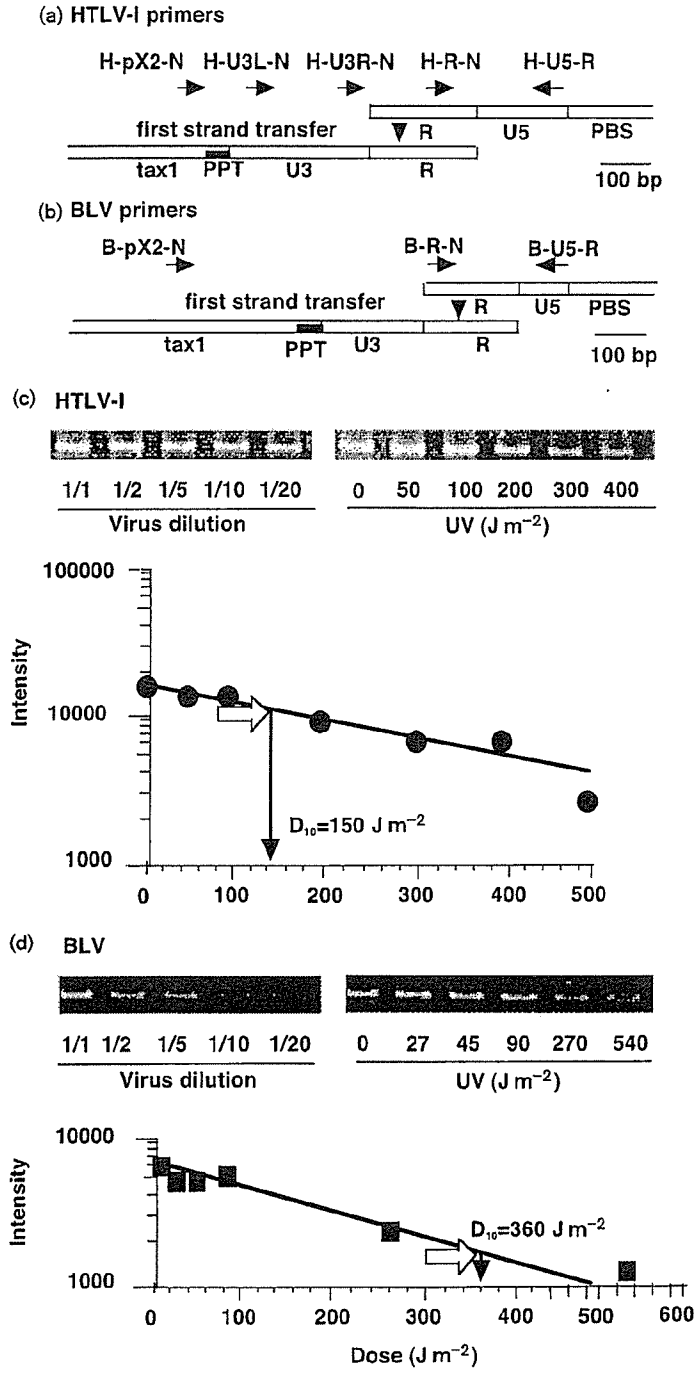

Fig. 5. UV sensitivity of the early stages of reverse transcription. PCR primers used in this experiment. (a) For HTLV-I, we used the antisense primer H-U5-R and four sense primers to examine PCR products of different lengths. The polypurine tract (PPT) is located in the *tax1* gene before the *U3* gene. (b) For BLV, we used the antisense primer B-U5-R and two sense primers. A 100 bp scale bar is shown. (c)–(d) Detection of viral DNA formation after infection of UV-irradiated viruses. 8C cells were infected with diluted or UV-irradiated HTLV-I_{MEL5} (c) and BLV (d) and cultured for 24 h. Viral DNA was detected by using PCR (HTLV-I, 37 cycles; BLV, 33 cycles) using the HTLV-I primers H-pX2-N and H-U5-R and the BLV primers B-pX2-N and B-U5-R. PCR fragment sizes were calculated to be 823 bp. The left five lanes were obtained using virus dilutions from 1/1 to 1/20. The right six lanes are irradiation doses, from 0 to 400 J m^{-2} for HTLV-I_{MEL5} and from 0 to 540 J m^{-2} for BLV. Densitometry of the PCR bands. The open arrows show the intensities that 1/10 diluted viruses gave and the closed arrows show D_{10} values. D_{10} values for HTLV-I and BLV were estimated to be 150 and 360 J m^{-2}, respectively.

single-stranded RNA genomes of a similar size, and they are closely related to each other among various retroviruses (Sagata *et al.*, 1984). However, we found that there was a marked difference in UV sensitivity between these two viruses. The UV sensitivity of BLV or MoMuLV determined by us was similar to those previously reported for BLV (Guillemain *et al.*, 1981) as well as for other retroviruses (Yoshikura, 1989). We showed here that there was nearly a 10-fold difference in the D_{10} values determined by the infectivity and the PCR assay, using the *gag* primer pairs between HTLV-I and BLV after the infection of irradiated cell-free HTLV-I and BLV. The sensitivity of HTLV-I to UV light was thus much higher than those of other retroviruses, and was accordingly similar to those of other RNA viruses.

There seems to have been no report describing the effect of UV irradiation on several phases of the progression of reverse transcription. Under our assay conditions for PCR,

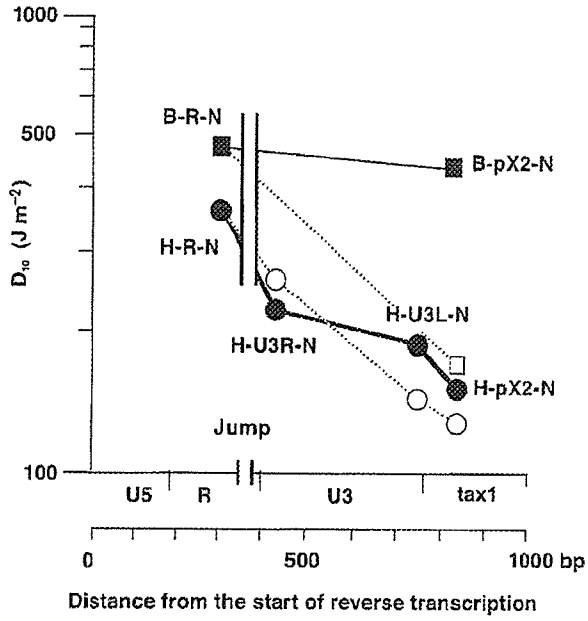

Fig. 6. D_{10} values determined using the PCR primers shown above. The horizontal axis shows the distance from the start of reverse transcription. Experiments were repeated at least twice and mean D_{10} values were plotted. Open symbols with dotted lines represent D_{10} values calculated based on the assumptions described in the legend of Fig. 4 and in the text: HTLV-I but not BLV gave values near the expected values. Symbols: ● and ○, HTLV-I; ■ and □, BLV.

PCR bands would be detected once a negative-strand DNA is formed by reverse transcription. We showed that the D_{10} values determined by infectivity (syncytium formation assay) and viral DNA formation (PCR that will detect negative-strand DNA formation using the *gag* PCR primer pair) were similar (Table 1). This finding suggests that retroviruses are inactivated by UV because their negative-strand DNA is not completely synthesized.

As a target, putative UV-sensitive viral structures have already been mentioned in the literature. Lovinger *et al.* (1975) examined the UV sensitivity of reverse transcriptase and concluded that at least 5–10 % of the loss of infectivity in irradiated retrovirus preparations may be due to viral polymerase inactivation. Owada *et al.* (1976) examined the UV inactivation of avian sarcoma virus and concluded that inactivation is caused not only by RNA damage but also damage in RNA–protein linkage as well as polymerase inactivation. Henderson *et al.* (1992) studied HIV-1 and stated that the formation of dimers (uracil dimers) after UV-irradiation alone is not effective for virus inactivation, because reverse transcriptase has the ability to read through the damaged bases. The nucleotide, including the linear sequence as well as its secondary or tertiary structures, has been supposed to be a major target for UV inactivation. However, reports on RNA photobiology are very limited. It has been supposed that the formation of pyrimidine hydrates and cyclobutadipyrimidines is important in the UV inactivation of RNA viruses, as it is for DNA viruses (Murphy & Gordon, 1981).

There has not been an easy assay to quantify the infectivity of cell-free HTLV-I therefore, we used a new method that we established recently, where we could detect the formation of syncytia 1 week after infection of Tax-1-expressing 8C cells by cell-free HTLV-I. The D_{10} values of two cosmopolitan (Japanese) strains, 2M and MT-2, and one Melanesian strain, MEL-5, of HTLV-I were about 20 J m^{-2} by this method. The D_{10} of VSV determined using a plaque formation assay was 6 J m^{-2}. Thus, HTLV-I was still more UV-resistant than VSV.

We thought of the possibility that, if an irradiated virus infects cells, which harbour part of the viral gene, the D_{10} obtained would be higher than the actual value. If so, we would not be able to determine an accurate D_{10} when we used target cells that have previously been transfected with a viral gene. Therefore, if we use 8C/Tax1 cells that contain the *tax1* gene, the D_{10} of HTLV-I would be observed to be higher than the real D_{10} determined using cells without the *tax1* gene. However, the D_{10} of HTLV-I in our experiments was still very low. Since the UV sensitivity determined by PCR using 8C cells not transfected with the *tax1* gene (Figs 3–6) was similar to that determined by the infectivity assay using 8C/Tax1 cells, we concluded that the transfection of target cells by the *tax1* gene did not greatly influence the results of UV inactivation of HTLV-I.

As shown in Figs 4 and 6, the difference in UV sensitivity between HTLV-I and BLV was already observed at a very early stage of reverse transcription or before formation of the strong-stop DNA. Thus, this stage of the reverse transcription of HTLV-I RNA was already very sensitive to UV. We constructed chimeric MoMuLVs that contained 823 bp fragments of the HTLV-I or BLV origins and tested their UV sensitivities. We could hardly detect any difference in UV sensitivity between the two chimeric MoMuLVs. This result suggests that the primary RNA sequence itself is not a determinant of the high UV sensitivity of HTLV-I.

It is expected that there will be an inverse relationship between the UV target size of RNA or DNA and the corresponding D_{10} when the UV target is homogeneously sensitive to damage induced by UV irradiation: (value of D_{10}) × (target genome size) = constant. We examined whether this was true for HTLV-I and BLV. The D_{10} values determined by infectivity assays of HTLV-I and BLV were about 17 and 180 J m^{-2}, respectively (Fig. 1a; Table 1); the target sizes of UV irradiation are about 8·5 kb. Thus, D_{10} values for the UV target size of 300 bp are calculated to be about 480 and 5100 J m^{-2} for HTLV-I and BLV, respectively, whereas the experimental values were 370 and 480 J m^{-2}, respectively (Table 1). For HTLV-I, there was a good correlation between experimentally obtained values and calculated values while, for BLV, there

was an apparent discrepancy, as shown in Figs 4 and 6. This finding suggests that HTLV-I is susceptible to UV damage according to its target RNA size, while UV-irradiated BLV genomes may not be damaged proportionally to their genome sizes.

Several possibilities to explain the difference in UV sensitivity between HTLV-I and BLV can be suggested: (i) the genomic RNA sequence of HTLV-I contains more UV-sensitive sequences, for example pyrimidine dimers, than that of BLV, (ii) the abilities of the reverse transcriptases of HTLV-I and BLV to read through UV-damaged lesions are different, (iii) the first-strand transfer (jump) step of HTLV-I is especially vulnerable to UV irradiation, (iv) the virion structures of HTLV-I and BLV are different, especially the nucleocapsid (NC) and RNA complex structures or (v) recombination between RNA genomes in virions takes place much more readily during reverse transcription of BLV than of HTLV-I.

The first possibility seems unlikely, as we showed that chimeric MoMuLVs harbouring the HTLV-I and BLV *tax1-LTR* regions of 823 bp were similarly resistant to UV irradiation. Their D_{10} values were about 420 J m^{-2}, similar to that of the parental MoMuLV strain, suggesting that a factor(s) other than linear RNA sequence may be responsible for the difference in UV sensitivity. Even in the case of RNA, pyrimidine dimers have been thought to be a major target of UV irradiation (Murphy & Gordon, 1981). Therefore, we counted the pyrimidine dimers in HTLV-I and BLV as well as MoMuLV, and found that HTLV-I and BLV had quite similar patterns of pyrimidine dimer constitution (data not shown).

The second possibility also seems unlikely because UV-irradiated VSV RNA similarly functioned as a template to make cDNA using reverse transcriptase of either HTLV-I or BLV (data not shown). Figs 4 and 6 showed that the first-strand transfer (jump) step did not markedly affect the reverse transcription efficiency of HTLV-I and BLV.

A recent report by Morcock *et al.* (2002) suggested that the fourth possibility cannot be ruled out. Morcock *et al.* (2002) examined the affinity of NC proteins of retroviruses for their RNA: an NC protein of HTLV-I, p15, is more than 100-fold more loosely associated with HTLV-I RNA than NC proteins of other retroviruses, for example BLV, HIV-1 or simian immunodeficiency virus. Namely, there is a possibility that reverse transcriptase can read through UV-damaged viral RNA more readily if viral RNA is tightly associated with NC protein. Another possibility may be that RNA tightly associated with NC protein is less vulnerable to UV irradiation than that loosely associated with NC protein, like HTLV-I RNA. The D_{10} of BLV was still smaller than that of HIV-1, as reported by others (Yoshikura, 1989) and according to the report by Morcock *et al.* (2002). NC protein of BLV is still less tightly associated with viral RNA than that of HIV-1. These findings seems to favour the fourth possibility.

Lastly, the recombination of virus genomes during reverse transcription could partly explain the results obtained for BLV. Retroviruses contain two equivalent RNA genomes in their virions. It has been reported that chimeric viruses are readily made in retroviruses when cells are infected with different types of virus (Telesnitsky & Goff, 1997). If recombination between two virus genomes in the same virions takes place during reverse transcription, UV-damaged lesions in one RNA strand may be rescued by the other intact strand. Even if this is the case, HTLV-I should lack this recombination ability, since its UV sensitivity can be explained by its target genome size, as shown in Figs 4 and 6. In contrast, other retroviruses, including BLV, may have this activity.

We showed that, among the retroviruses examined so far, HTLV-I had the most UV-sensitive infectivity and that the reverse transcription of all the regions of the HTLV-I genome was similarly sensitive to UV irradiation, whereas there was a discrepancy between the UV target size of the BLV genome and its sensitivity to UV irradiation. The mechanisms underlying these observations remain to be investigated further. Our findings may be helpful to solve an old question: why are retroviruses so resistant to UV irradiation?

ACKNOWLEDGEMENTS

We thank Drs G. Nolan, R. Yanagihara and D. G. Blair for kindly supplying us with Phoenix-E cells, HTLV-I_{MEL5}-producing SI-5 cells and PG-4 cells, respectively. This work was supported in part by a Grant-in-Aid from the Japanese Society for the Promotion of Science, and grants from the Japan Health Sciences Foundation and CREST.

REFERENCES

Akagi, T., Nyunoya, H. & Shimotohno, K. (1991). Murine retroviral vectors expressing the *tax1* gene of human T-cell leukemia virus type 1. *Gene* **106**, 255–259.

Bogdanov, K. V., Chukhlovin, A. B., Zaritskey, A. Y., Frolova, O. I. & Afanasiev, B. V. (1997). Ultraviolet irradiation induces multiple DNA double-strand breaks and apoptosis in normal granulocytes and chronic myeloid leukemia blasts. *Br J Haematol* **98**, 869–872.

Clapham, P., Nagy, K. & Weiss, R. A. (1984). Pseudotypes of human T-cell leukemia virus types 1 and 2: neutralization by patients' sera. *Proc Natl Acad Sci U S A* **81**, 2886–2889.

Fan, N., Gavalchin, J., Paul, B., Wells, K. H., Lane, M. J. & Poiesz, B. J. (1992). Infection of peripheral blood mononuclear cells and cell lines by cell-free human T-cell lymphoma/leukemia virus type I. *J Clin Microbiol* **30**, 905–910.

Fischinger, P. J., Peebles, P. T., Nomura, S. & Haapala, D. K. (1973). Isolation of RD-114-like oncornavirus from a cat cell line. *J Virol* **11**, 978–985.

Gessain, A., Barin, F., Vernant, J. C., Gout, O., Maurs, L., Calender, A. & de The, G. (1985). Antibodies to human T-lymphotropic virus type-I in patients with tropical spastic paraparesis. *Lancet* 24, 407–410.

Guillemain, B., Mamoun, R., Astier, T. & Duplan, J. F. (1981). Mechanism of early and late polykaryocytosis induced by the bovine leukaemia virus. *J Gen Virol* **57**, 227–231.

Haapala, D. K., Robey, W. G., Oroszlan, S. D. & Tsai, W. P. (1985). Isolation from cats of an endogenous type C virus with a novel envelope glycoprotein. *J Virol* **53**, 827–833.

Haraguchi, Y., Yang, D. W., Handa, A., Shimizu, N., Tanaka, Y. & Hoshino, H. (1994). Detection of neutralizing antibodies against human T-cell leukemia virus type 1 using a cell-free infection system and polymerase chain reaction. *Int J Cancer* **59**, 416–421.

Henderson, E. E., Tudor, G. & Yang, J. Y. (1992). Inactivation of the human immunodeficiency virus type 1 (HIV-1) by ultraviolet and X irradiation. *Radiat Res* **131**, 169–176.

Hinuma, Y., Nagata, K., Nanaoka, M., Nakai, M., Matsumoto, T., Kinoshita, K. I., Shirakawa, S. & Miyoshi, I. (1981). Adult T-cell leukemia: antigen in an ATL cell line and detection of antibodies to the antigen in human sera. *Proc Natl Acad Sci U S A* **78**, 6476–6480.

Hoshino, H., Shimoyama, M., Miwa, M. & Sugimura, T. (1983). Detection of lymphocytes producing a human retrovirus associated with adult T-cell leukemia by syncytia induction assay. *Proc Natl Acad Sci U S A* **80**, 7337–7341.

Hoshino, H., Clapham, P. R., Weiss, R. A., Miyoshi, I., Yoshida, M. & Miwa, M. (1985). Human T-cell leukemia virus type I: pseudotype neutralization of Japanese and American isolates with human and rabbit sera. *Int J Cancer* **36**, 671–675.

Hoshino, H., Nakamura, T., Tanaka, Y., Miyoshi, I. & Yanagihara, R. (1993). Functional conservation of the neutralizing domains on the external envelope glycoprotein of cosmopolitan and melanesian strains of human T-cell leukemia/lymphoma virus type I. *J Infect Dis* **168**, 1368–1373.

Jacobson, S., Raine, C. S., Mingioli, E. S. & McFarlin, D. E. (1988). Isolation of an HTLV-1-like retrovirus from patients with tropical spastic paraparesis. *Nature* **331**, 540–543.

Levinson, W. & Rubin, H. (1966). Radiation studies of avian tumor viruses and of Newcastle disease virus. *Virology* **28**, 533–542.

Lovinger, G. G., Ling, H. P., Gilden, R. V. & Hatanaka, M. (1975). Effect of UV light on RNA-directed DNA polymerase activity of murine oncornaviruses. *J Virol* **15**, 1273–1275.

Miyoshi, I., Kubonishi, I., Yoshimoto, S., Akagi, T., Ohtsuki, Y., Shiraishi, Y., Nagata, K. & Hinuma, Y. (1981). Type C virus particles in a cord T-cell line derived by co-cultivating normal human cord leukocytes and human leukaemic T cells. *Nature* **294**, 770–771.

Miyoshi, I., Yoshimoto, S., Taguchi, H., Kubonishi, I., Fujishita, M., Ohtsuki, Y., Shiraishi, Y. & Akagi, T. (1983). Transformation of rabbit lymphocytes with T-cell leukemia virus. *Gann* **74**, 1–4.

Morcock, D. R., Katakam, S., Kane, B. P. & Casas-Finet, J. R. (2002). Fluorescence and nucleic acid binding properties of bovine leukemia virus nucleocapsid protein. *Biophys Chem* **97**, 203–212.

Murphy, T. M. & Gordon, M. P. (1981). Photobiology of RNA viruses. In *Comprehensive Virology, Methods Used in the Study of Viruses*, vol. 17, pp. 285–349. Edited by H. Fraenkel-Conrat & R. Wangeer. New York: Plenum.

Nagy, K., Clapham, P., Cheingsong-Popov, R. & Weiss, R. A. (1983). Human T-cell leukemia virus type I: induction by syncytia and inhibition by patients' sera. *Int J Cancer* **32**, 321–328.

Osame, M., Usuku, K., Izumo, S., Ijuchi, N., Amitani, H., Igata, A., Matsumoto, M. & Tara, M. (1986). HTLV-I associated myelopathy, a new clinical entity. *Lancet* **3**, 1031–1032.

Owada, M., Ihara, S., Toyoshima, K., Sugino, Y. & Kozai, Y. (1976). Ultraviolet inactivation of avian sarcoma viruses: biological and biochemical analysis. *Virology* **69**, 710–718.

Poiesz, B. J., Ruscetti, F. W., Gazdar, A. F., Bunn, P. A., Minna, J. D. & Gallo, R. C. (1980). Detection and isolation of type C retrovirus particles from fresh and cultured lymphocytes of a patient with cutaneous T-cell lymphoma. *Proc Natl Acad Sci U S A* **77**, 7415–7419.

Sagata, N., Yasunaga, T., Ogawa, Y., Tsuzuku-Kawamura, J. & Ikawa, Y. (1984). Bovine leukemia virus: unique structural features of its long terminal repeats and its evolutionary relationship to human T-cell leukemia virus. *Proc Natl Acad Sci U S A* **81**, 4741–4745.

Soda, Y., Shimizu, N., Jinno, A., Liu, H. Y., Kanbe, K., Kitamura, T. & Hoshino, H. (1999). Establishment of a new system for determination of coreceptor usages of HIV based on the human glioma NP-2 cell line. *Biochem Biophys Res Commun* **258**, 313–321.

Telesnitsky, A. & Goff, S. P. (1997). Reverse transcriptase and the generation of retroviral DNA. In *Retroviruses*, pp. 144–145. Edited by J. M. Coffin, S. H. Hughes & H. E. Varmus. Cold Spring Harbor, NY: Cold Spring Harbor Laboratory.

Van der Maaten, M. J. & Miller, J. M. (1975). Replication of bovine leukemia virus in monolayer cell cultures. *Bibl Haematol* **43**, 360–362.

Yanagihara, R., Nerukar, V. R. & Ajdukiewicz, A. B. (1991). Comparison between strains of human T lymphotropic virus type I isolated from inhabitants of the Solomon Islands and Papua New Guinea. *J Infect Dis* **164**, 443–449.

Yoshikura, H. (1989). Thermostability of human immunodeficiency virus (HIV-1) in a liquid matrix is far higher than that of an ecotropic murine leukemia virus. *Jpn J Cancer Res* **80**, 1–5.

Available online at www.sciencedirect.com
SCIENCE DIRECT®
Biochemical and Biophysical Research Communications 313 (2004) 55–61
BBRC
www.elsevier.com/locate/ybbrc

Anti-HIV-1 activity and mode of action of mirror image oligodeoxynucleotide analogue of zintevir

Hidehito Urata,[a,*] Tetsuya Kumashiro,[a] Takuya Kawahata,[b] Toru Otake,[b] and Masao Akagi[a,*]

[a] *Osaka University of Pharmaceutical Sciences, 4-20-1 Nasahara, Takatsuki, Osaka, 569-1094, Japan*
[b] *Osaka Prefectural Institute of Public Health, 1-3-69 Nakamichi, Higashinari-ku, Osaka 537-0025, Japan*

Received 17 November 2003

Abstract

Zintevir is an oligonucleotide analogue, which has the phosphorothioate modification at both termini, that forms a K^+-induced quadruplex structure and shows potent anti-human immunodeficiency virus (HIV)-1 activity. We synthesized the non-modified analogue (D-17mer) of Zintevir and its enantiomer (L-17mer), and compared their anti-HIV-1 activity and molecular mechanism of action. Although L-17mer forms the exact mirror image quadruplex structure of D-17mer, which has a very similar structure with Zintevir, L-17mer showed comparable anti-HIV-1 activity with Zintevir. The results obtained by the time-of-addition experiments and the immunofluorescence binding assay strongly suggest that the primary molecular target of L-17mer is the viral gp120 envelope protein as well as Zintevir, regardless of their reciprocal chirality.

Keywords: Anti-HIV-1 activity; Chirality; DNA; Enantiomer; Viral entry; Zintevir

The chirality of molecules plays important roles in the higher structural organization and specific ligand recognition of biomolecules [1]. Usually, the enantiomer of a molecule shows different behavior and action from the parental molecule in chiral environment such as living body. Recent discovery of 2′-deoxy-3′-thiacytidine (3TC), which has an unnatural L-configuration, brought about a breakthrough in nucleoside-based chemotherapy of viral diseases. This antiviral nucleoside analogue (3TC) is discovered as a racemic compound [2]. Coats et al. separated each optical isomer of 2′-deoxy-3′-thiacytidine and they evaluated their anti-HIV-1 activity. Unexpectedly, the unnatural stereoisomer (3TC) showed comparable anti-HIV-1 activity with natural one, in spite of its unnatural configuration [3,4]. Moreover, 3TC showed an extremely lower cytotoxicity for host cells than the natural stereoisomer [3–5]. Therefore, 3TC should be recognized by HIV-1 reverse transcriptase after phosphorylation and taken into the growing DNA strand to inhibit the further elongation of the viral DNA strand, although phosphorylated 3TC should not be easily recognized by host cell polymerases [6]. This means that HIV-1 reverse transcriptase is unable to recognize 3TC with a stereospecific manner. In addition to HIV-1 reverse transcriptase, D-peptide containing the basic-arginine rich region of the Tat protein was reported to specifically bind to the major groove of TAR RNA in a similar fashion to that observed for the natural L-Tat peptide [7,8]. Above facts suggest that these proteins derived from HIV-1 may recognize their specific ligands with low or even no stereospecificity.

Zintevir	d(G*TGGTGGGTGGGTGGG*T)
D-17mer	d(GTGGTGGGTGGGTGGGT)
L-17mer	L-d(GTGGTGGGTGGGTGGGT)

*: phosphorothioate linkage

Zintevir (T 30177) is a guanosine-quartet structure (G-tetrad)-forming single stranded oligodeoxynucleotide (Fig. 1), which is partially phosphorothioated at both the termini to raise its in vivo stability. Zintevir was discovered as a potent inhibitor for HIV-1 integrase [9,10], and this discovery seemed to promise the

* Corresponding authors. Fax: +81-72-690-1005.
E-mail addresses: urata@gly.oups.ac.jp (H. Urata), akagi@gly.oups.ac.jp (M. Akagi).

0006-291X/$ - see front matter © 2003 Elsevier Inc. All rights reserved.
doi:10.1016/j.bbrc.2003.11.094

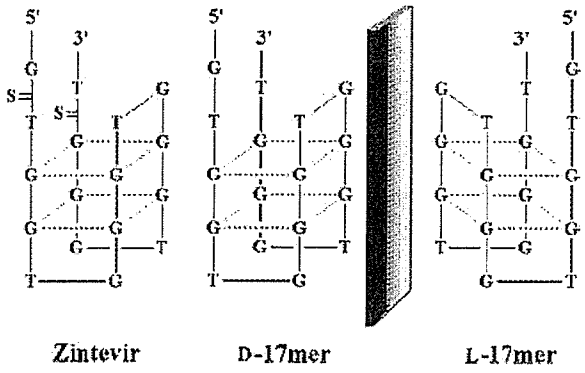

Fig. 1. Structures of Zintevir, D-17mer, and L-17mer.

development of antiviral agents directed to a novel target of HIV-1 replication. Recently, the primary molecular target of Zintevir, however, was shown to be the HIV-1 gp120 envelope protein by the genetic analysis of the Zintevir-resistant strain, in which the resistant phenotype was associated with the emergence of mutations in the gp120 protein [11]. In this paper, to verify whether the rationale that HIV-1-related proteins recognize nonstereospecifically their specific ligands is also compatible to other viral proteins or not, we synthesized the all-phosphodiester analogue (D-17mer) of Zintevir and its mirror image 17mer (L-17mer) as well as Zintevir. Since oligonucleotides having an unnatural L-configuration show nearly complete resistance towards nucleases [12,13], L-oligonucleotide should have a more preferable properties as an antiviral agent than natural D-oligonucleotides. Here, we report the synthesis, physico- and biochemical characterization of the enantiomer (L-17mer) of Zintevir, and also its action mechanism associated with the anti-HIV-1 activity.

Materials and methods

General methods. L-Thymidine, L-deoxyguanosine, and their phosphoramidites were synthesized by the previously reported procedures [12,13]. Reagents for the DNA synthesizer other than L-thymidine and L-deoxyguanosine phosphoramidites were purchased from Applied Biosystems Japan (Tokyo, Japan). MALDI-TOF mass analyses of the 17mers were carried out on a PE Biosystems Voyager Linear DE or Elite spectrometer. Nuclease P1 and SVPD were purchased from Yamasa (Chiba, Japan) and Roche Diagnostics (Mannheim, Germany), respectively.

Synthesis of oligodeoxynucleotides. Oligodeoxynucleotides were synthesized by an Applied Biosystems model 392 DNA/RNA synthesizer. After usual deblocking, the purification was performed on a column of MonoQ HR 5/5 (Amersham Bioscience) with a linear gradient of NaCl in 10 mM NaOH by a Shimadzu LC-10A HPLC system. After neutralization, samples were desalted with Sep-Pak Plus C18 cartridge (Waters). The purity of the 17mers tested by the above system was more than 95%. The structures of the 17mers were confirmed by MALDI-TOF MS spectra: Zintevir, $C_{170}H_{210}O_{103}N_{70}P_{16}S_2$ calcd. *m/z* 5438.86 [M$^-$]; found 5439.84 (negative), D-17mer, $C_{170}H_{210}O_{105}N_{70}P_{16}$ calcd. *m/z* 5405.90 [M$^+$]; found 5406.66 (positive), and L-17mer, $C_{170}H_{210}O_{105}N_{70}$ P_{16} calcd. *m/z* 5405.90 [M$^+$]; found 5407.19 (positive).

Resistance against nuclease digestion. A solution (3 ml) of each 17mer (3OD units) containing 50 mM ammonium acetate (pH 5.0) for nuclease P1 or 10 mM $MgCl_2$, 50 mM Tris–HCl (pH 8.0) for SVPD was placed in a 1 cm path-length quartz cell. With stirring at 37 °C, enzyme (nuclease P1, 1 mg/ml, 2 μl; SVPD, 2 mg/ml, 2 μl) was added into the solution, and absorbance at 260 nm was measured for 3 h by a JASCO Ubest-55 spectrophotometer equipped with a temperature controller.

Measurements of CD spectra. A solution (4 μM) of each 17mer containing 20 mM lithium phosphate (pH 7.0) and designated concentration of KCl was placed in a 1 cm path-length quartz cell. Spectra were measured by a JASCO J-820 spectropolarimeter equipped with a temperature controller.

Cells and virus. MT-4 and Molt-4 cell lines, which are human leukemic T-cell lines, were maintained in RPMI-1640 (Nikken Biomedical Laboratory, Kyoto Japan) supplemented with 10% fetal calf serum (FCS), 100 U/ml penicillin, and 100 μg/ml streptomycin. HIV-1_{LAI} strain was obtained from culture fluid of Molt-4 cells persistently infected with HIV-1_{LAI} strain.

Anti-HIV-1 activity assay. MT-4 cells were infected with HIV-1_{LAI} strain at a multiplicity of infection (MOI) of 0.001 for 1 h and washed once with the culture medium mentioned above. The infected MT-4 cells were suspended in a culture medium containing inhibitors, which had been diluted stepwise, at a concentration of 1.5×10^5 cells/ml. The suspension was cultured at 37 °C for five days. Viable cell count was determined by the trypan blue dye exclusion methods and the 50% inhibitory concentration (IC_{50}) for each virus stock was calculated.

Time-of-addition experiments. At MOI of 0.5, HIV-1 was allowed to adsorb to 2×10^5 MT-4 cells in the absence or presence of the inhibitors (10 μM) on ice for 60 min. The cells were washed with cold culture medium three times to remove unadsorbed virus and then incubated at 37 °C. The inhibitors were added at 10 μM concentration at different times (0–6 h) after infection, as shown in Fig. 5. Some cells were harvested for PCR assay 12 h after virus inoculation.

Immunofluorescence binding assay. As many as 1×10^6 uninfected MT-4 cells were reacted with monoclonal antibody against CD4 (FITC-labeled anti-Leu3a antibody: Becton–Dickinson Immunocytometry Systems, San Jose, CA, USA) at 37 °C for 30 min in the absence or presence of the inhibitors (100 μM). The cells were washed three times with 0.15 M PBS and then re-suspended in PBS containing 3% formaldehyde. A pair of anti-HIV-1 gp120 V3 (0.5β) [14] and Molt-4 cells persistently infected with HIV-1 was reacted in the same manner as described above. The cells were washed three times with 0.15 M PBS and then reacted with anti-mouse IgG1 antibody labeled with FITC (Research Diagnostics, Flanders, NJ, USA) at 37 °C for 30 min. The cells were washed three times with 0.15 M PBS and then re-suspended in PBS containing 3% formaldehyde. The fluorescence intensity of the suspension was measured using a flow cytofluorometer (Epics XL, Beckman Coulter, Fullerton, CA, USA) and the percentage of the fluorescence intensity of inhibitor-treated cells relative to that of untreated cells as a positive control was calculated.

Results and discussion

Synthesis and structure of 17mers

L-Thymidine, L-deoxyguanosine, and their phosphoramidites were synthesized by the previously reported procedure [13]. Synthesis of an L-oligodeoxynucleotide was achieved by the same methodology as that of D-oligodeoxunucleotides according to the conventional

solid-phase phosphoramidite chemistry. Since guanine-rich sequences, which show heterogeneity in their structure by intra- and inter-molecular hydrogen-bonding interactions, provide some difficulty in the purification step, we employed an anion exchange column with alkaline conditions for the purification of the 17mers. The chemical structures of the 17mers were confirmed by MALDI-TOF MS spectra.

In the presence of K^+ cations, Zintevir has been reported to effectively form an intramolecular G-tetrad structure [9,10]. To confirm the tertiary structure of L-17mer, circular dichroism (CD) spectra were measured. The positive Cotton band at around 265 nm of Zintevir is dramatically strengthened by increasing K^+ cation concentration, suggesting the formation of the stable G-tetrad structure, and the spectra of D-17mer under both low and high K^+ concentration conditions are very similar to those of Zintevir. On the other hand, L-17mer shows the same CD strength and the same behavior by increasing K^+ cation concentration as D-17mer except for its sign (Fig. 2). These results strongly suggest that L-17mer has the mirror image tertiary structure of D-17mer and Zintevir. Fig. 3 shows the temperature dependence of the CD strength at 260 nm of the 17mers at 0.2 M K^+ cation concentration. All the 17mers show the structural transition from the G-tetrad structure into a random coil by increasing temperature, whose midpoints are higher than 80 °C. Thus, all the 17mers similarly form the highly stable G-tetrad structure under these conditions.

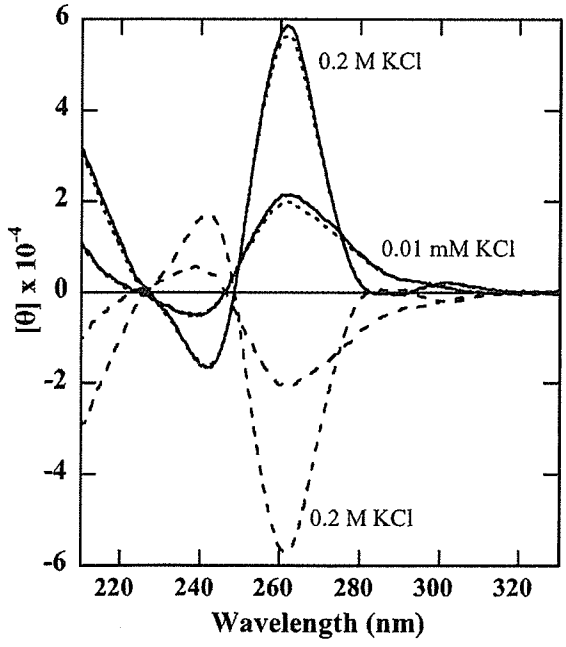

Fig. 2. CD spectra of Zintevir (solid lines), D-17mer (dotted lines), and L-17mer (broken lines) in 20 mM lithium phosphate (pH 7.0) containing 0.2 M or 0.01 mM KCl at 25 °C.

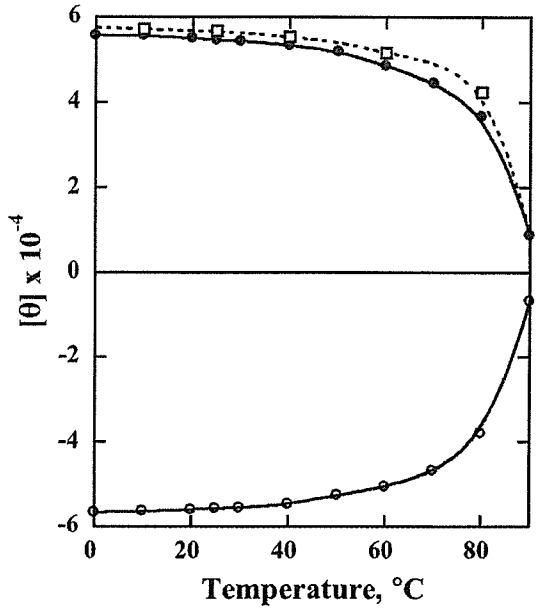

Fig. 3. Temperature dependence of molar ellipticity at 260 nm of Zintevir (open square), D-17mer (closed circle), and L-17mer (open circle) in 20 mM lithium phosphate (pH 7.0) containing 0.2 M KCl.

Anti-HIV-1 activity and nuclease resistance

Zintevir has been shown to possess potent anti-HIV-1 activity [9,10]. To evaluate the anti-HIV-1 activity of L-17mer, the in vitro inhibitory effects of the 17mers on the HIV-1-induced cytopathicity in MT-4 cells were tested. The inhibitory effects of Zintevir and L-17mer were almost the same, their IC_{50} values being 0.225 μM, despite having opposite chirality to each other, whereas that of D-17mer is 0.57 μM. The difference in the activity between the two former 17mers and the latter one was considered to be due to the difference of their resistance to nucleases in the culture medium and/or in the cells. Therefore, we compared the susceptibility of the 17mers towards snake venom phosphodiesterase (SVPD) and nuclease P1. Fig. 4 shows the time course of hyperchromicity at 260 nm induced by degradation of the 17mers with the enzymes. D-17mer was degraded rapidly with both of the enzymes. Under the same conditions, Zintevir showed significant resistance for SVPD, which is a 3′-exonuclease, yet not so much for nuclease P1 (Figs. 4A and B, respectively), because of its phosphorothioate modification at both termini. In contrast, L-17mer was completely resistant to both of the enzymes under the same conditions. Therefore, the lower anti-HIV-1 activity of D-17mer may be due to its susceptibility to degradation by nucleases.

Time-of-addition experiments

Although Zintevir has been reported to inhibit viral integrase, the primary molecular target of Zintevir was

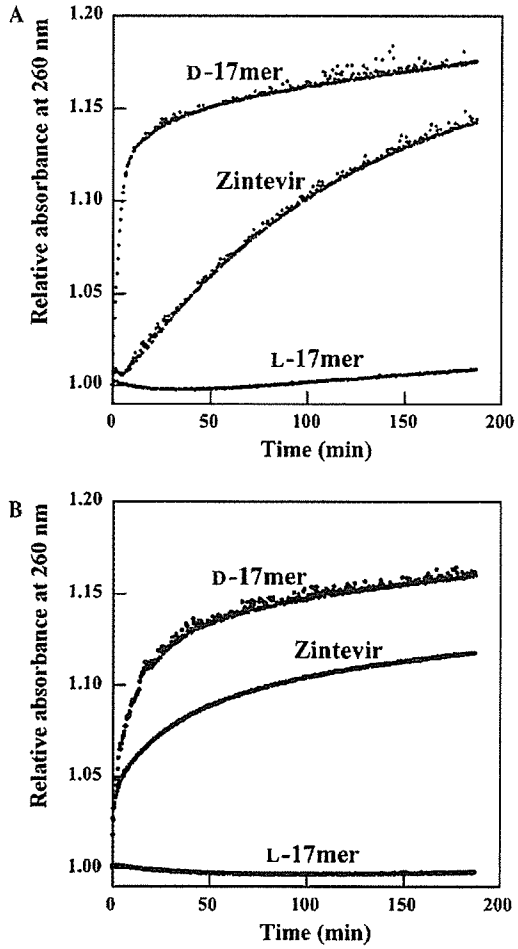

Fig. 4. Resistance of the 17mers against SVPD (A) and nuclease P1 (B). Reactions started by adding enzyme into the buffered solution of each 17mer at 37 °C. Hyperchromicity at 260 nm induced by degradation of an oligonucleotide is revealed periodically.

recently shown to be the viral gp120 envelope protein [11]. To verify the inhibitory step(s) of L-17mer within the HIV life cycle, time-of-addition experiments [15] were conducted, whereby the 17mers were added at different times after exposure of the MT-4 cells to HIV-1. In this assay system, the viral *gag* gene integrated into the host cell DNA can be observed by the electrophoresis when the 17mers cannot exhibit their inhibitory effects. The result is shown in Fig. 5. Zintevir could not show any inhibitory potency when it was added at 2 h or later after viral infection (lanes 14–16). However, when Zintevir was present only during the viral adsorption step, and also when virus-adsorbed cells were started to culture in the presence of Zintevir, it showed the inhibitory potency (lanes 12 and 13, respectively). Inhibition by AZT decreased when it was added at 4 h after viral infection (data not shown). This result strongly suggests that Zintevir inhibits the viral adsorption onto the host cells and the entry into the cells as reported by Esté et al. [11]. Similarly, D-17mer and L-17mer were

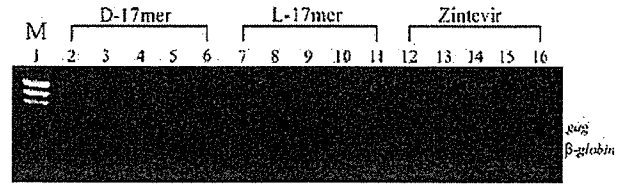

Fig. 5. Time-of-addition experiments for the 17mers. HIV-1 was adsorbed onto MT-4 cells on ice and the mixture was allowed for 1 h at this temperature in the presence or absence of each 17mer (adsorption). After free virus was washed out with ice-cold buffer, incubation was started at 37 °C and the 17mers were added after the designated incubation time as below. After 12 h, cells were harvested and amplified the viral *gag* gene together with the host *β-globin* gene by PCR: lane 1, size marker; lanes 2, 7, and 12, each 17mer existed only during the "adsorption" step; lanes 3, 8, and 13, each 17mer was added when the incubation started; lanes 4, 9, and 14, each 17mer was added at 2 h after the start of the incubation; lanes 5, 10, and 15, each 17mer was added at 4 h after the start of the incubation; lanes 6, 11, and 16, each 17mer was added at 6 h after the start of the incubation.

effective when they were present only during the viral adsorption step (lanes 2 and 7, respectively), and also when virus-adsorbed cells were started to culture in the presence of them (lanes 3 and 8, respectively). However, they lost their inhibitory activity if the treatment was delayed until 2 h after infection. (lanes 4 and 9, respectively). This strongly suggests that the inhibitory step of L-17mer is viral adsorption and/or viral entry within the HIV replicative cycle as well as Zintevir and D-17mer.

Immunofluorescence binding assay

Both viral envelope proteins and cellular receptors are closely related to the viral adsorption and entry process, and are considered as a candidate for the molecular target of the 17mers. To verify this point, the immunofluorescence binding assay was conducted. Zintevir had no effect on the binding of a monoclonal antibody against the gp120-binding domain of CD4 (anti-Leu3a) to the CD4 cellular receptor of MT-4 cells (Fig. 6C), whereas it significantly inhibited the binding of monoclonal antibody (0.5β) [14] (directed to an epitope in the V3 loop region of gp120) to MOLT-4 cells persistently infected with HIV-1_{LAI} (Fig. 7C). These results strongly suggest that Zintevir binds not to the CD4 receptor but to the gp120 viral envelope protein, and thus the results support the conclusion of Esté et al. obtained by the genetic analysis of the Zintevir-resistant strain of HIV-1 [11]. Similarly, D- and L-17mers showed the inhibitory effects for the binding of anti-gp120 mAb (0.5β) to MOLT-4 cells (Figs. 7D and E, respectively), but not for the binding of anti-CD4 mAb (anti-Leu3a) to the CD4 cellular receptor of MT-4 cells (Figs. 6D and E, respectively). The above findings suggest that the primary molecular target of L-17mer would be the viral gp120 protein as well as Zintevir, although both 17mers have the opposite chirality to each other.

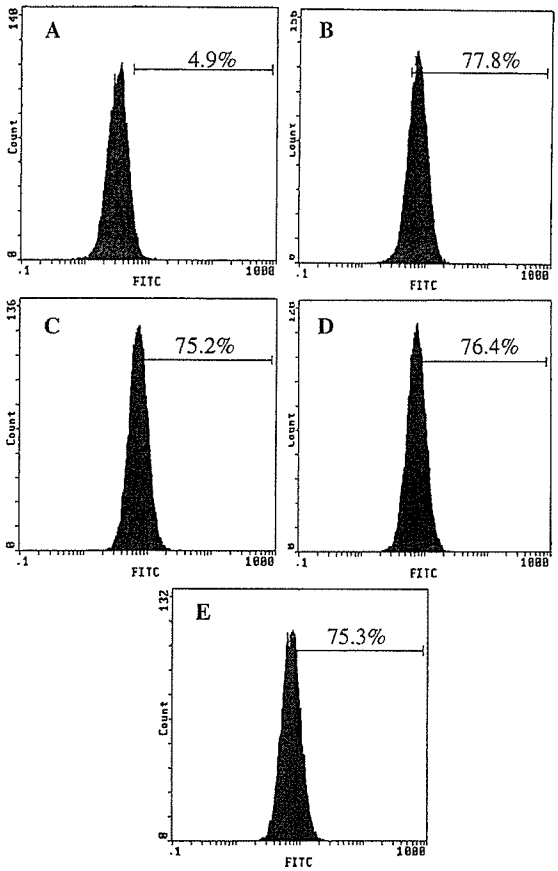

Fig. 6. Flow cytometric histograms of the binding of anti-CD4 mAb (Leu3a) on MT-4 cells: (A) fluorescence of MT-4 cells incubated only with FITC-labeled anti-mouse IgG1 antibody; (B) fluorescence of MT-4 cells incubated with anti-CD4 mAb (Leu3a), then with FITC-labeled anti-mouse IgG1 antibody; (C,D,E) fluorescence of the cells incubated as (B) in the presence of Zintevir, D-17mer, and L-17mer (100 μM each), respectively.

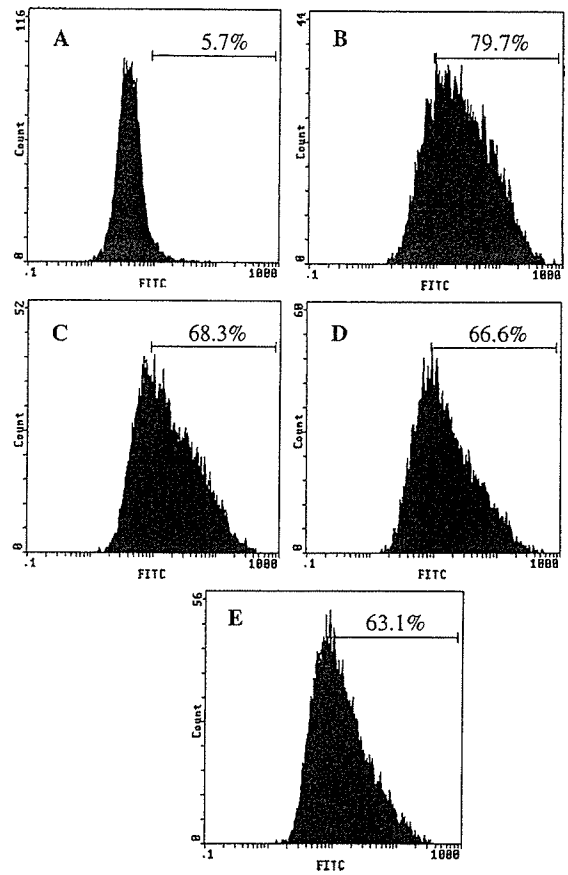

Fig. 7. Flow cytometric histograms of the binding of anti-gp120 mAb (0.5β) on Molt-4 cells persistently infected with HIV-1_{LAI}: (A) fluorescence of Molt-4 cells incubated only with FITC-labeled anti-mouse IgG1 antibody; (B) fluorescence of Molt-4 cells incubated with anti-gp120mAb (0.5β), then with FITC-labeled anti-mouse IgG1 antibody; (C,D,E) fluorescence of the cells incubated as (B) in the presence of Zintevir, D-17mer, and L-17mer (100 μM each), respectively.

Generally, chiral biomolecules show a strict enantiospecificity toward their substrates and ligands. Recently, some cases, in which L-nucleotides are recognized by natural enzymes, have been shown, such as T4 DNA ligase [16], human and viral deoxynucleoside kinases [17,18], viral reverse transcriptases [19,20], and HIV-1 integrase [21]. From a chemotherapeutic point of view, viral proteins that are recognized by L-nucleic acids are attractive molecular targets, since L-nucleic acid-based drugs can be expected to have the enhanced biological stability and the reduced cytotoxicity. Zintevir possesses the phosphorothioate modification at both the termini to raise its in vivo stability. This modification for oligonucleotides is also applied for antisense molecules, but it has been reported to cause nonspecific binding to some proteins, which should lead to undesirable side effects [22]. The toxicity of Zintevir should be partly owing to such nonspecific binding to some proteins. In contrast, L-17mer has no such modification and is expected to have superior chemotherapeutic nature to Zintevir.

Although Zintevir has been developed as a potent inhibitor for HIV-1 integrase, which was thought to be possibly associated with the anti-HIV-1 activity, the primary molecular target of Zintevir was shown to be the viral gp120 protein by the genetic analysis of Zintevir-resistant strain [11]: yet, there is a possibility that Zintevir also inhibits the later stage(s) of the HIV-1 replicative cycle. In the time-of-addition assay described here, we could not observe such activities for L-17mer as well as Zintevir and D-17mer. This result not only confirms the conclusion of Esté et al. [11] that the primary target of Zintevir is the viral adsorption and fusion, both of which are mediated in part by gp120, but also suggests that L-17mer inhibits these stages to exhibit the anti-HIV-1 activity. Zintevir was reported to be internalized by cells during prolonged incubation and it takes 4–6 h that the intracellular concentration of Zintevir reaches the extracellular levels [23]. Although integration of viral DNA starts at around 6–9 h after the viral infection [24], we could not observe intracellular